



Laing, Stacey and Jamieson, Lauren E. and Faulds, Karen and Graham, Duncan (2017) Surface-enhanced Raman spectroscopy for in vivo biosensing. Nature Reviews Chemistry, 1. ISSN 2397-3358 , <http://dx.doi.org/10.1038/s41570-017-0060>

This version is available at <https://strathprints.strath.ac.uk/61920/>

Strathprints is designed to allow users to access the research output of the University of Strathclyde. Unless otherwise explicitly stated on the manuscript, Copyright © and Moral Rights for the papers on this site are retained by the individual authors and/or other copyright owners. Please check the manuscript for details of any other licences that may have been applied. You may not engage in further distribution of the material for any profitmaking activities or any commercial gain. You may freely distribute both the url (<https://strathprints.strath.ac.uk/>) and the content of this paper for research or private study, educational, or not-for-profit purposes without prior permission or charge.

Any correspondence concerning this service should be sent to the Strathprints administrator: strathprints@strath.ac.uk

Surface enhanced Raman spectroscopy for *in vivo* biosensing

Stacey Laing,[#] Lauren E. Jamieson,[#] Karen Faulds and Duncan Graham

Centre for Molecular Nanometrology, WestCHEM, Department of Pure and Applied Chemistry, Technology and Innovation Centre, University of Strathclyde, 99 George Street, Glasgow, G1 1RD, United Kingdom

[#]Both authors contributed equally to this work.

Correspondence to D.G.: duncan.graham@strath.ac.uk

Abstract | Surface enhanced Raman scattering (SERS) is of interest for biomedical analysis and imaging due to its sensitivity, specificity and multiplexing capabilities. The successful application of SERS for *in vivo* biosensing necessitates probes to be biocompatible and procedures to be minimally invasive, challenges that have respectively been met by the design of nanoproboscopes and instrumentation. This Review presents recent developments in these areas, describing case studies in which sensors have been implemented, as well as outlining shortcomings that have to be addressed before SERS sees clinical use.

In 1928, C. V. Raman first reported the scattering phenomenon that now bears his name.^{1,2} Raman scattering has since become a powerful analytical technique, including for biomedical applications,³ where label-free and objective tissue diagnostics⁴⁻⁶ *ex vivo* and *in vivo*, as well as drug-cell interaction studies *in vitro* have been conducted.⁷⁻⁹ The majority of incident photons experience elastic (Rayleigh) scattering, with only about 1 in 10⁷ photons undergoing inelastic (Raman) scattering.¹⁰ In 1974, Fleischmann and co-workers described a phenomenon that would later become known as surface enhanced Raman scattering (SERS)¹¹. They observed a large enhancement in inelastic scattering from pyridine when the analyte was adsorbed onto a Ag electrode, an effect that had previously been mentioned by the team of A. J. McQuillan in 1973,¹² with Van Duyne later attributing the signal enhancement to the roughened metal surface *via* the physical phenomenon he coined SERS.¹³ Unlike conventional Raman spectroscopy, SERS analyses require samples to be labelled, a disadvantage offset by the large intensity enhancement that makes SERS an important analytical tool with high sensitivity and low detection limits.^{14,15} The exact mechanism of SERS is not fully understood but an electromagnetic enhancement factor plays the major role¹⁶, whereby free electrons in a metal nanoparticle (NP) encounter applied radiation whose electromagnetic field varies at a frequency matching the oscillation frequency of electrons in the NPs. Such plasmon resonance at the NP surface arises from an intense electric field, which intensifies Raman modes arising from molecules near or attached to the NP surface. The Raman signals can also be enhanced due to the formation of charge-transfer complexes between the roughened metal surface and molecules bound to it. We now leave our discussion of the SERS mechanism, but refer readers interested in these fundamental principles to some comprehensive articles on the subject.¹⁷⁻¹⁹

Well-known selection rules allow for one to predict if a given vibrational mode is infrared- and/or Raman-active. Indeed, by considering the magnitude of the change in dipole moment or polarizability associated with a vibration, one can rationalize infrared or Raman data, respectively. Compared to Raman spectroscopy, SERS involves analyte molecules interacting with a roughened metal substrate, such that the symmetry of the system, and thus the selection rules, are now unclear.¹⁶ Moving from Raman to SERS, this adsorption or complexation of the molecules to the surface can result in peaks appearing or disappearing, peak intensities changing dramatically, and peak broadening. Molecules can also orient themselves in a variety of ways relative to the metal surface, with different orientations giving rise to different SERS spectra. One requirement for SERS, which is the reason a roughened rather than a smooth metal surface is required, is a polarizability component perpendicular to the metal surface. Different orientations of the same molecule have different polarizability components parallel and perpendicular to the surface, and may thus have stronger or weaker SERS as a result. In terms of analyte functionality, π -conjugated systems tend to possess strong Raman scattering cross sections due to their distributed electron clouds that can be easily polarized in the presence of an electric field.

The unique characteristics of SERS have motivated investigations applying the technique in biosensing and biomedical contexts, with the majority of these reports describing analyses of *in vitro* and *ex vivo* biofluid samples. Since the first SERS characterization of an organic compound in 1984,²⁰ many studies have focused on the detection of oligonucleotide sequences or proteins in biofluid samples with a view to diagnosing diseases. Accordingly, SERS-based immunoassays were realized in 1989,²¹ followed by a SERS-based gene probe in 1994²². SERS has major advantages over the (primarily fluorescence-based) biological assays in use, with the former being potentially more sensitive and more amenable to multiplexed measurements — those in which multiple analytes are detected simultaneously. The latter is possible because SERS signals are typically much sharper than fluorescence peaks. The first SERS detection of two different DNA sequences was reported in 2000²³, with more recent work extending this to six oligonucleotide sequences²⁴, as well as, in 2014, the first quantitative multiplexed bioassay²⁵. SERS probes have also been used for *in vitro* studies, in which interactions between small molecules and cells can be studied with a view to screen and develop drugs.^{26,27} In addition to biofluid samples, immuno-Raman microspectroscopy has been used for antigen detection on tissue samples for disease diagnosis²⁸; this, and other major advances in SERS sensing are depicted in Figure 1.

Although SERS has found extensive use for *in vitro* and *ex vivo* analyses, its incorporation into *in vivo* bioanalytical methods has proven more difficult. This Review will describe studies towards this lofty goal, as well as outlining the technological challenges still faced by those undertaking such research. Indeed, SERS has yet to be adopted in a clinical setting for detecting analytes in human subjects, and significant optimization will be required for us to realize the benefits of this distinct technique. In the 43 years since its discovery in 1974, it took 15 years for SERS to be applied in the context of a biological assay in 1989,²¹ and 32 years before its application *in vivo* in 2006.²⁹ Despite not yet being applied for *in vivo* analysis in the clinic, SERS has seen success in an *ex vivo* platform, with the Fungiplex assay for detection of 12 different fungal pathogens, developed by Renishaw Diagnostics, being released for clinical application in 2015.³⁰⁻³² This came 26 years after the first report of a SERS based biological assay. It stands to reason that the next 15 years could prove crucial for advancing *in vivo* SERS diagnosis in the clinic, with this year being only 11 years after the first application of SERS in an animal model *in vivo*.

In the sections that follow, this Review will address two major concerns associated with *in vivo* SERS measurements: nanosensor design and instrument selection and optimization. SERS makes use of metal NPs and is thus not considered a ‘label-free’ technique. Although NPs have been used in medical applications such as imaging and photothermal therapy (PTT),³³ the toxicity of NPs is a major concern associated with moving SERS *in vivo*. Despite this, there is substantial evidence for the biocompatibility of NPs (particularly those of Au), with some already having been approved for use in other clinical settings. Before focusing on SERS developments exclusively, it is important to be aware of other methods, including spontaneous Raman, as well as the nonlinear techniques coherent anti-Stokes Raman spectroscopy (CARS) and stimulated Raman spectroscopy (SRS). The vigour of efforts aimed at bringing SERS to the clinic is matched by the impetus behind these three methods, which have an obvious advantage over SERS in that they are label-free such that their biocompatibility rests only on the degree of laser exposure required. These alternative methods give rise to weaker signals (that is, they are less sensitive) and although there are overlaps in the applications of the techniques, each can be seen as having a particular clinical application. Spontaneous Raman spectroscopy has been applied *in vivo* for clinical applications, which involve a monochromatic laser interrogating the tissue site and scattered Raman photons being detected. This technology has already been used on human subjects for skin care,^{34,35} the diagnosis of cervical³⁶ or bladder cancer,³⁷ gastrointestinal endoscopy,³⁸ breast cancer tumour resection,³⁹ and brain tumour resection.⁴⁰ In 2016, BBC News notably reported the use of a Raman probe in surgery for real-time imaging of tumour boundaries during a brain tumour resection.⁴¹ In spontaneous Raman spectroscopy, the discrimination between cancerous and non-cancerous tissue generally relies on complicated and robust machine-learning models that often discriminate based on very small spectral differences. Given that spontaneous Raman spectroscopy does not need a label, relative to SERS it has fewer safety considerations and has

found greater success in the clinic. With SERS, one not only needs to meet International Standards for laser exposure, but also consider the toxicology hurdle surrounding NP application *in vivo*. Once this is surmounted, there is vast scope for improved detection. Research into clinical spontaneous Raman spectroscopy has given rise to commercially available products such as the skin-cancer-sensing Verisante “Aura” probe,^{42,43} which is adaptable to nanoprobe and thus will also help make *in vivo* SERS a reality.

We view the prospect of having a ‘yes or no’ response according to the presence or absence of a SERS spectrum as being a clean and simple detection method, one that could be translated into a simple colour or sound response to the clinician. Although SERS has recently been applied to *in vivo* imaging, we believe that the major strength of SERS is its sensitivity, possible because the data feature strong SERS enhancement and minimal background signal, which can be rapidly converted to a ‘yes or no’ response for one or multiple markers. Vast efforts have been made to use spontaneous Raman for objective *ex vivo* diagnosis of tissue sections, this method being an alternative to standard histology protocols that rely on subjective analysis by a trained pathologist.⁵ Raman has yet to emerge victorious here, and must also compete against Fourier transform infrared spectroscopy, a much faster method. SERS has also been used for diagnosis in tissue sections *ex vivo*²⁸ but there is a more equal push towards the *in vivo* detection capabilities of SERS. The primary advantage of CARS and SRS over spontaneous Raman is speed. Being nonlinear techniques, CARS and SRS allow rapid image acquisition, although they only probe one vibrational transition rather than a spectral range. Therefore, their applications are highly focussed on real-time structural and dynamic data acquisition of carefully selected vibrational transitions of native biological species.⁴⁴⁻⁴⁷

On considering the examples described above, it would appear that cancer detection is the most prominent application for *in vivo* Raman spectroscopies. Yet, SERS has also found use in the continuous monitoring of glucose levels in diabetic patients. Spontaneous Raman spectroscopy would be much less amenable to this use, which requires the selective detection of one specific molecule in a complex biological environment. The high sensitivity required is not well met by the weak nature of spontaneous Raman scattering. On the other hand, SERS probes can be designed that selectively bind to glucose and enhance its signals, and indeed there are applications in which SERS is superior to spontaneous Raman techniques.⁴⁸ Like any technique, SERS has its pitfalls, and work is continuously being undertaken to, for example, address the binding of poorly selective glucose probes that also bind other sugars with similar structures. For example, the use of non-targeting and targeting probes allows specific and non-specific binding to be discerned during cancer detection,⁴⁹ and more sophisticated nanoprobe have improved glucose selectivity.⁵⁰

We are hopeful that the full benefits of SERS will be realised in the coming years, as the technique continues to be pushed further towards *in vivo* clinical use. Despite only 11 years having passed since the first *in vivo* study, many promising studies have already surfaced, including some in glucose sensing^{29,48,51} and cancer diagnosis.^{52,53} These key advances will be discussed, as will applications to other diseases. In addition to diagnostics, SERS has been used for intraoperative guidance for tumour removal,⁵⁴ and, when in combination with drug delivery and PTT, enables targeted tumour detection and treatment.⁵⁵ We will highlight prominent examples in these areas, describing the challenges that have already been overcome, as well as those that still need to be addressed before these analytical tools find clinical use.

[H1] Nanosensor design

To observe a SERS signal, a Raman-active molecule must be adsorbed onto, or lie in close proximity to, a roughened metal surface. Although one can directly detect analytes such as biomolecules,^{56,57} a typical procedure involves using a strongly absorbing dye or a Raman reporter molecule with an affinity for the metal surface and a large Raman cross section, so that further enhancement can be achieved.⁵⁸⁻⁶⁰ The application of the metal NPs and Raman reporter *in vivo* can come only after careful consideration of their properties. The toxicity of NPs has consequently been studied extensively and has been the subject of detailed reviews.⁶¹⁻⁶⁵ Briefly, the toxicity and biocompatibility of NPs is largely dependent on their size, shape, charge and surface chemistry,⁶⁶⁻⁶⁹ as well as other

factors such as their propensity to aggregate.⁷⁰ Each of these properties must be carefully considered when designing nanosensors for *in vivo* applications and toxicological effects must be assessed when fabricating or altering probes for bioanalysis. As we noted above, Au NPs are considered relatively safe (certainly more so than Ag NPs), and can be made even safer upon protective coating. As long as one keeps in mind the particle properties and dosage, Au NPs show good biocompatibility and are suitable for application *in vivo*, although not before detailed investigations into the effects these NPs have on cells. Long-term changes in cells following exposure to Au NPs under different conditions can lead to changes in gene expression of the cells⁶⁹. Although Au NPs have generally been found to be non-cytotoxic, with negligible changes in cell viability or proliferation following exposure, small changes in morphology and gene regulation can occur, these being more apparent for acute rather than chronic NP exposure.⁶⁹ This is relevant to the use of NPs for biosensing in that exposure would generally be in an acute dose. The interactions that NPs have with cells depend both on the NP surface — which may or may not be coated — as well as the cell type. In addition to considering the toxicity of the metal NPs and the overall biocompatibility of the SERS-active probes, it is crucial that the whole sensor remains intact *in vivo* to produce the desired signal, after which the NPs should be promptly expelled from the body. Furthermore, it is essential that a SERS signal can be obtained using laser wavelengths that are safe and suitable *in vivo*. For these reasons, many factors have to be considered when building a nanosensor for biomedical applications. These design principles and the technologies that best satisfy them are depicted in Figure 2.

[H3] *SERS substrates.* Au and Ag NPs have been the traditional choices when it comes to signal-enhancing metal surfaces for SERS. This is partly due to the energies of their surface plasmon resonance (SPR) absorption bands, which lie in the visible region and are conveniently probed by readily available lasers. *In vivo* SERS applications will benefit instead from excitation in the near infrared (NIR) region, as the background signals from tissues and biomolecules are much weaker in this region⁷¹. Additionally, NIR light induces less photodegradation and penetrates tissue more deeply, which is beneficial for *in vivo* detection. The optical properties of NPs are readily tuneable by varying their size, shape and chemical composition. Consequently, extensive research has been undertaken to design SERS substrates with localised surface plasmon resonances (LSPRs) in the NIR region and to investigate whether or not the substrates provide an improved SERS enhancement. These materials can take the form of solid surfaces modified with signal-enhancing metal layers or films,⁷²⁻⁷⁴ or colloidal suspensions of particles with varying size and shape. For most *in vivo* applications, the latter are more suitable since NP solutions can simply be injected into live animals, whereas the solid support requires implantation. Despite this, solid SERS-active substrates are useful for certain biomedical applications, and can be incorporated into glucose-sensing implants.^{72,75} AgNPs afford strong SERS signals, although the toxicity of Ag NPs remains a concern for *in vivo* applications.⁷⁶⁻⁷⁸ AuNPs are more biocompatible, give rise to more reproducible signal intensities and have surfaces that are more easily functionalized for bioconjugation.⁷⁹ Additionally, Au nanostructures tend to exhibit LSPRs at longer wavelengths, rendering them more suitable for use with NIR-SERS. Therefore, the majority of *in vivo* applications involve the use of Au as the enhancing metal substrate.

Thin metal nanoshells, when encircling a dielectric core, can feature a plasmon band whose energy is tuneable from UV to NIR by altering the core diameter and shell thickness.⁸⁰⁻⁸² Indeed, by carefully adjusting the diameter of a SiO₂ core and the thickness of an Au shell surrounding it, the SPR can be tuned from 800 nm to around 1060 nm in order to match the wavelengths of NIR Raman lasers.⁸² NIR-SERS has also made use of Au/Ag alloy shells,^{83,84} the synthesis of which involves a redox reaction between dissolved [AuCl₄]⁻ and a Ag template.⁸⁵ Each SiO₂ nanosphere is coated by many such hollow Au/Ag shells, and the composite can be injected into live animals, in which they enable multiplexed detection using NIR-SERS⁸⁴. The diameter of the hollow shell centre and the Au:Ag atomic ratio can be varied to red-shift plasmon bands from $\lambda_{\text{max}} = 480$ to 825 nm. The Au/Ag shells that cover the SiO₂ core have been further encapsulated in a SiO₂ shell, and samples of the material have been functionalized with three different Raman chromophores. Each of the three nano-assemblies (“NIR SERS dots”), along with a mixture of all three, were injected into different sites in a mouse and intense Raman signals were obtained for all three reporters upon 785 nm laser excitation.

Additionally, peaks from each of the Raman reporters appeared in the spectrum of the mixed sample, which may thus represent a useful nanoprobe for *in vivo* multiplexed detection.

In addition to the metal shells described above, in which a hollow Ag sphere is surrounded by a layer of Au, one can also prepare hollow Au nanoshells (HGNs) by depositing Au with concomitant oxidation of a Co template. The resulting spherical particles are small (50 – 80 nm), and tuning the core diameter and shell thickness gives control over the LSPR properties of relevance to NIR-SERS.⁸⁶⁻⁸⁹ When the concentrations of the reactants are optimized, the HGNs are relatively well-defined, with particle diameters of 78.7 ± 22.5 nm and shell thicknesses in the range 8.8 ± 1.34 nm⁹⁰. These particles are smaller than earlier HGNs and gave an effective SERS response at 1064 nm (a common wavelength for a Nd:YAG laser) when functionalised with seven different Raman reporters. Consequently, they have shown significant potential for human cell or tissue analysis and would be particularly suitable for *in vivo* applications such as PTT.⁹¹

As well as the spherical particles discussed thus far, rod-⁹²⁻⁹⁵ and star-shaped nanostructures⁹⁶⁻¹⁰⁰ also have optical properties that make them appropriate for use as NIR-SERS substrates, including for *in vivo* applications. Au nanostars have been used in Raman imaging for the detection of tumours of various cancer types at different stages. The success of this methodology, which uses experimental conditions similar to those used in a clinical setting⁹⁶, arise from the exceptional specificity and sensitivity of the SERS nanostars, which afforded a detection limit of the nanostars as low as 1.5 fM. Raman imaging was also carried out *in situ*, signifying the potential application of this system for intraoperative detection. Au nanostars have also proven useful for *in vivo* NIR-SERS analysis of animal tumours using transdermal detection, using 785 nm laser irradiation at powers that would be acceptable for human skin⁹⁷. The method also allowed for nanostars to be detected when embedded in *ex vivo* human skin graft samples or when dispersed in a biocompatible hydrogel as a carrier matrix. Lastly, SERS-encoded nanostars can be embedded in a tissue-integrating polymer scaffold and implanted into live rats and pigs, in which signals from the probes could be detected. Spectra could also be obtained from the pig over a period of 6 days using a handheld Raman system, without the need for anaesthesia, further demonstrating the versatility of this detection method for clinical applications.

It is not essential that the LSPR frequency of the SERS substrate matches the laser frequency, but we reiterate that significant efforts have been made to develop substrates suited to excitation at longer wavelengths, with such radiation penetrating tissue more deeply and giving rise to less intense background signals. Additionally, apart from tuning substrate LSPR and size, the most useful materials are biocompatible such that they are suitable for a variety of biomedical applications, from detection and imaging, to drug delivery and PTT.

[H3] *Functionalizing the substrate.* Although NIR lasers are preferred for *in vivo* SERS applications, Raman scattering of these long wavelengths is intrinsically weak. Therefore, as well as selecting the most suitable metal substrate, one must choose a Raman reporter molecule that significantly enhances SERS at these wavelengths. A good SERS reporter molecule will produce a strong Raman signal and have an affinity for the metal surface. Therefore, Raman reporters often possess π -conjugated systems, due to their distributed electron clouds, and functional groups such as thiols, isothiocyanates or amines for surface attachment. Additionally, further enhancement can be obtained by incorporating a chromophore as the Raman reporter, and selecting a laser excitation wavelength which matches an electronic transition of the chromophore, resulting in resonance Raman scattering with enhancement in signal of up to 10^6 being achievable. Further, if multiplexed detection is desired, then each reporter should exhibit distinct spectral features that are easily resolved.^{101,102} Fluorophores²⁵, UV-vis dyes,¹⁰³ as well as non-resonant aromatic reporters¹⁰⁴ are all useful in terms of their high scattering efficiencies. However, alternative molecules with improved NIR sensitivity and strong affinity for suitable metal substrates have also been investigated as potential SERS reporters. A selection of 80 tricarbocyanine reporters with varying amine structures were used in combination with AuNPs for NIR-SERS at 785 nm laser excitation.⁵³ Those consisting of mostly aromatic amines gave the most intense SERS signals, with CyNAMLA-381 yielding a 12-fold increase in sensitivity relative to the

commonly used 3,3'-diethylthiatricocyanine (DTTC) reporter molecule. One can move truly in the NIR region by instead using chalcogenopyriliium dyes, 14 different examples of which were loaded on separate HGN samples. These dyes possess a range of absorption maxima from 653 nm to 826 nm, varying substituents which give unique Raman spectra and they each possess multiple S or Se groups which allow strong adsorption onto the Au surface for maximum SERS enhancement. In each case, excitation with a 1280 nm laser afforded intense and unique SERS spectra with detection limits ranging from 1.5 ± 0.1 – 32.8 ± 2.4 pM for 12 of the 14 dyes¹⁰⁵. It was elucidated that the dye which gave the strongest SERS signal did so because of its significantly red-shifted absorption maxima of 826 nm, making it NIR-active, and the presence of the selenophene groups, which result in stronger binding to the Au surface than the alternative thiolates. SERS of the same dyes with spherical Au and Ag NPs was significantly weaker, and no SERS signal at all could be observed when the common NIR-Raman reporters 1,2-bis(4-pyridyl)ethylene or 4,4'-azopyridine were combined with HGNS and irradiated at 1280 nm. This highlights the importance of specifically designing nanotags for a particular excitation wavelength, as well as the correct combination of SERS substrate and Raman reporter. Even more sensitive than the examples above are thiophene-substituted chalcogenopyriliium dyes, with these NIR Raman reporters enabling a detection limit of 100 aM¹⁰⁶. They were also applied for *in vivo* tumour imaging, and their unique fingerprint spectra make them suitable for the detection of multiple markers *in vivo*. More recent work describes two new chalcogenopyriliium dyes with absorption maxima at 959 and 986 nm, which, when used with 100 nm AuNPs and excited at 1550 nm, gave intense SERS spectra with detection limits of 50.6 ± 4.6 and 62.9 ± 4.8 pM, respectively.¹⁰⁷ Achieving such sensitivity using a retina-safe laser is particularly impressive since Raman scattering is inherently weak in this NIR region, yet is advantageous for biomedical applications.

Certain examples of NIR-active cyanine dyes not only give rise to SERS but also allow for simultaneous photoacoustic (PA) imaging¹⁰⁸. Strong SERS and PA signals were observed from a chloro-substituted Cy7 dye, of which one indole can be tethered to a lipoic acid residue to anchor the dye to AuNPs. Covalent attachment allows for robust and reproducible Raman scattering, and the nanoprobe can then be encapsulated in poly(ethylene glycol) (PEG) to enhance their stability and aqueous solubility. The coated nanoprobe was dosed into cells, which exhibited close to 100% viability and were thus subjected to *in vivo* SERS detection and PA imaging. In addition, nanoprobe could also be further labelled with an antibody that increases the selectivity of the particles for cancer cells over healthy cells. Both SERS and PA analyses indicated that accumulation of probes in a tumour is maximized after 6 hours and 24 hours for the labelled and unlabelled nanoprobe, respectively. The particles also accumulated in the liver and spleen, but, encouragingly, they are excreted from the mice after ~72 hours. Combining PA imaging with SERS detection allows deep penetration for successful tumour identification, as well as excellent sensitivity to help ensure one can find and remove even small tumours. More generally, the development of biocompatible probes for multimodal imaging is extremely useful for *in vivo* biosensing because the limitations of each technique can be overcome by combining their advantages.

Careful design of SERS substrates and reporters enables one to continually lower the detection limits for biological species. Indeed, sensitivity is one of the most important factors when designing new diagnostic tests, as early detection of disease improves patients' prognoses. In terms of sensitivity, SERS measurements can be superior to fluorescence-based measurements *in vivo*,¹⁰⁹ and the former offer greater multiplexing capabilities and specificity due to the unique fingerprint spectra arising from specific molecular vibrations. Certain reporter molecules, such as DTTC, can be utilised for dual-mode imaging using both SERS and fluorescence. One can favour either SERS or fluorescence by modifying the distance between the reporter and the metal surface. Multilayer-coated Au nanorods, functionalized with DTTC, have tuneable optical properties. Their fluorescence allows one to quickly identify potential areas of interest, such as tumour sites, while the sharp SERS signals from the DTTC allow a more accurate localization of the tumours, particularly because the signals were significantly more intense from the specific sites where NPs had accumulated⁹⁴. This combination of techniques is extremely useful but also highlights the potential SERS has *in vivo*, where a specific signal, with little to no background signal from other regions, can be obtained from an area of interest. This level of

specificity is of utmost importance in moving towards clinical applications where a clear-cut distinction between a healthy and diseased state is essential.

As we have seen, the properties of a SERS substrate and reporter molecule are paramount in obtaining SERS signals *in vivo*. It is also important that the SERS nanoprobe finds its way to the desired location before its signal is measured. Although passive targeting is suitable in certain *in vivo* applications, more commonly employed is active targeting, in which the nanoprobe is functionalized with a recognition moiety. This moiety, which may take the form of an antibody,¹⁰⁹ aptamer¹¹⁰ or folic acid,¹¹¹ allows more sensitive detection of specific antigens *in vivo*. A lot of *in vivo* SERS-based biosensing research has focused on cancer detection, in which nanotags are functionalised with antibodies specific to antigens — such as epidermal growth factor receptor (EGFR) and human epidermal growth factor 2 (HER2) — that are overexpressed in tumours.^{52,53} Of course, this targeted approach is not unique to cancer imaging, and a wide range of antibodies specific to other diseases are commercially available. For example, antibody-conjugated Au NPs allow *in vivo* detection of intercellular adhesion molecule 1 (ICAM-1), an inflammation marker of many inflammatory, autoimmune and infectious diseases¹⁰⁹. By attaching a Raman reporter, 2,2-dipyridyl, to Au NPs, coating them with a SiO₂ shell and functionalizing them with a ICAM-1-specific antibody, one obtains specific SERS signals *in vivo* with double the sensitivity of two-photon fluorescence. Again, this highlights the sensitivity of SERS, which is unparalleled by other analytical methods.

As was alluded to above, *in vivo* applications call for nanosensors to be coated, such that their biocompatibility, stability, resistance to aggregation, and SERS signal are enhanced, the latter on account of the reduced desorption of the Raman reporters once trapped inside the coating. The protective coating may also be made to include functional groups that allow subsequent conjugation to targeting molecules. Various approaches have been investigated for the encapsulation of SERS nanoprobe, and coatings such as polymers,¹¹²⁻¹¹⁴ SiO₂,¹¹⁵⁻¹¹⁷ proteins,⁵³ PEG^{108,118,119} and chitosan^{120,121} have been explored. One particular type of ‘all-in-one’ NP coating is NIR dye-loaded poly(N-(2-hydroxypropyl)methacrylamide) (pHPMA), the terminal thiol of which binds AuNPs to afford NIR-SERS-active probes (Au@IR-pHPMA).¹¹² Aside from having a built-in dye, the polymer coating improves biocompatibility and *in vivo* stability of the AuNPs, increasing intravascular circulation times such that a strong SERS signal is observed even over 24 hours. In contrast to SiO₂ coatings, the ‘all-in-one’ coating affords small particles (< 20 nm) that can still be readily functionalized. These nanoprobe enabled *in vivo* imaging of lymph nodes, and, when three different probes were used, allowed for multiplexed analysis.

[H1] Optimizing instrumentation

In vivo SERS relies not only on the effectiveness of probes but also the efficiency of instrumentation, particularly in terms of portability, durability, cost, and ease of use for non-specialists. Common instrument configurations for Raman and SERS analysis include simple point-and-shoot devices, plate readers and more advanced mapping instruments. However, none of these configurations are optimized for *in vivo* measurement, for which specific devices are required. One of the primary considerations when designing a SERS instrument for *in vivo* sensing is obtaining a signal from a SERS substrate deep inside a body. Many early *in vivo* SERS studies were performed in rat or mouse models using mapping instruments with a configuration optimised to obtain signals from SERS probes subcutaneously. For example, a large 20 × 200 μm spot can be generated using a Renishaw inVia Raman microscope with a 12× open field lens and defocused beam¹²². The high numerical aperture objectives used for standard mapping experiments focus the laser into a small spot, limiting the time that the beam can be focused on a single location before damaging the sample. This limits the number of scattered photons detectable from that spot due to diffuse scattering from tissue. Instead, if a defocused beam with a larger spot size is used, one can obtain maximum signal from the SERS probes in the relevant tissue. Granted, using larger spot sizes lowers spatial resolution, but this is less of a problem in mapping applications, for which one is not so much concerned with detailed imaging but rather whether or not a positive or negative SERS response is rapidly obtained from a particular region. These mapping instruments, popular largely due to their availability to researchers studying these probes, are typically used for high resolution mapping experiments, such as *in vitro* cell and *ex*

vivo tissue analyses, but for *in vivo* SERS studies their highly spatially resolved mapping capabilities are largely not required and therefore more optimally designed instrumentation would be beneficial.

A rapid, dedicated small animal Raman imaging (SARI) instrument has been developed to image subjects after dosing them with nanoprobe¹²³. In contrast to previous *in vivo* Raman systems, SARI is optimised for rapid imaging of larger areas, for which the high image resolution capabilities of commercial systems are not required. The SARI system uses a line-scanning setup and a 2D electron-multiplying charge-coupled device (EMCCD) detector, and does not require the sample to be translated in *x* and *y* direction, because the laser is raster scanned along *x* and *y*. The capabilities of the SARI system for multiplexed imaging of four nanoprobe injected in living mice, were compared to the performance of the commercial Renishaw inVia system operating in Streamline mode. SARI is an order of magnitude faster at imaging, with an area of 5 mm × 5 mm being imaged in 1.5 min on SARI and 15 min on the inVia system. The SARI system imaged with a spatial resolution of 250 × 64 μm and a detection limit of 3.1 pM. It may prove difficult to apply the SARI instrument to larger animals — ultimately humans — because larger areas may need to be imaged and nanoprobe will potentially be more deeply buried within the body. The depth penetration of the SARI system was <4 mm, a figure that could be increased by combination with spatially offset Raman spectroscopy. For SERS to see clinical use we will need still further improvements in penetration, a problem that is being addressed using fibre optic endoscopic probes and surface enhanced spatially offset Raman scattering (SESORS) probes, which we now describe.

Endoscopic probes are widely used by pathologists, who analyse video images and can identify potentially cancerous lesions, for example, in the gastrointestinal tract (FIG. 3a,b). Efforts have been made towards developing a fibre-optic Raman endoscopic probe that would allow SERS detection of cancerous tissue, a more objective analysis that typically makes use of NPs designed to target a cancer-specific antigen. For example, a fibre-based Raman device insertable through a clinical endoscope is capable of multiplexed detection of up to ten labelled SERS nanoprobe with excellent sensitivity.¹²⁴ The fibre-optic bundle consists of a single-mode illumination fibre for 785 nm illumination, and 36 multimode fibres for collection. The highest laser power used was 42 mW, with the integration time being 300 ms, figures that are within the maximum permissible exposure (MPE) level for clinical use set out by the American National Standards Institute (ANSI). Under these conditions, the NPs themselves could be detected down to 440 fM, although this has also been interpreted in terms of a detection limit of a specific target receptor where the nanoparticles are functionalized with a receptor targeting ligand. Approximately 400 targeting ligands could be appended onto each nanoprobe, allowing for the target receptor to be detected at < 1 fM, with similar fluorescence-based endoscopic strategies only being useful down to 10 fM¹²⁵. Thus, the SERS method has superior sensitivity, as well as the capability of multiplexed detection of up to ten nanoprobe using a single monochromatic laser beam. In comparison, multiplexing with fluorescence is difficult due to the breadth of emission spectra, and the requirement to excite with multiple laser wavelengths. The SERS endoscope has already been approved and demonstrated for clinical use, and the hurdle that remains in the approval of the nanoprobe for clinical use. Significantly, topical application of nanoprobe prior to colonoscopy improved delivery of NPs to the desired site and reduced toxicity.¹²⁶⁻¹²⁸ In a robust study using over 120 mice, it was found that intrarectal topical application caused the NPs to localise on the colon only, with most never crossing to the systemic circulation before being excreted from the subjects after 24 hours. In contrast, intravenous injection proves more toxic, resulting in the NPs accumulating in the liver and spleen for prolonged time periods.

More recently, a device has been reported that allows both fluorescence and Raman detection, representing a dual modality system that can be inserted in a clinical endoscope for simultaneous fluorescence and SERS detection of HER2 and EGFR from breast cancer tumours¹²⁹. The nanoprobe are first located by looking for intense fluorescence, and then multiplexed detection of the two protein analytes is possible due to the sharp Raman bands of the rhodamine- and fluorescein-based dyes. The method is also applicable to esophageal cancer, with multiplexed detection of HER2 and EGFR being possible after topical application of targeted SERS NPs and detection with an endoscopic probe.¹³⁰ These studies demonstrated the suitability for *in vivo* SERS-based cancer detection in relation to

gastrointestinal tract cancers, which can be easily surveyed using endoscopic systems with Raman modality. Any tissues accessible to an endoscope could be probed in this manner, including skin, bladder, stomach, lungs, esophagus, cervix and vagina, and with many of the endoscopic Raman probes being approved for clinical use, the major barrier to surmount for this approach now surrounds nanoprobe toxicity. Many of these studies deploy nanoprobes topically, which circumvents dangers associated with nanoprobes entering the circulatory system, and is also advantageous compared to intravenous injection, which often results in that the probe accumulating in the liver and spleen. In related work, a unique endoscopic opto-electro-mechanical Raman device has been developed that allows rapid imaging of large tissue surfaces during gastrointestinal endoscopy by adding a rotating mirror between the collimating lens and tissue (FIG. 3a–d)¹³¹. They demonstrated the use of this endoscopy in phantoms, *ex vivo* porcine colon, and *in vivo* swine (FIG. 3a) for multiplexed detection of SERS nanoprobes. Images generated by the device could be displayed in both 2D and 3D, and background signal could be used to generate a 3D topography (FIG. 3c). This device allows large areas of hollow organs to be imaged rapidly and translated to an image easily interpretable by a physician, a vital aspect in clinical adoption of this technique.

SESORS is a new technique that overcomes the problems associated with detecting SERS from nanosensors implanted in tissue samples, far from the laser source and detector (FIG. 3e,f). Subcutaneous detection of SERS sensors buried in tissue is difficult due to loss of signal as a result of photons being scattered by the tissue. SESORS overcomes this problem by collecting scattered light in regions different from where the light was incident on the sample (FIG. 3e). In a standard Raman instrument, light is collected from the same point as the incident light, and this gives the greatest signal response from the surface of the sample. By collecting at regions of the sample offset from the position of the incident light, signals from deeper within the sample become predominant. This technique was first demonstrated using a transmission SESORS setup that could detect signals from nanoparticles buried 25 mm into a tissue sample¹³². In another study, four different SERS nanoparticles, located up to 50 mm within the sample, could be measured in tissue (FIG. 3f)¹³³. The first example of targeted SESORS imaging in bone, used bis(phosphonate)-tagged nanoparticles to localize at bones and be detectable even through 20 mm of porcine muscle tissue¹³⁴. In a more recent study, Sharma *et al.*¹³⁵ have also demonstrated the capability of SESORS to obtain SERS signals through bone. SESORS could be vitally important for translating SERS analysis into an *in vivo* environment, allowing subcutaneous measurements to be obtained, particularly where the tissue site is not accessible by an endoscopic probe.

Although the instruments discussed so far tend to be limited to use in a specialist clinical environment, and are designed primarily for detection of specific disease markers, it may be desirable to develop a portable, user-friendly and cheap instrument. These considerations are particularly important to enable SERS probes to be used in blood glucose sensing, in which a diabetic patient would ideally be able to continuously monitor their blood glucose level with a device worn on the body. Raman instruments — including handheld devices — are becoming increasingly advanced, yet none are optimized for glucose sensing. Therefore, although SERS appears a promising approach to monitor such biological markers, there is a need for efforts in instrument design to follow suit and allow analytical advances to be of use to patients.

[H1] Key advances in *in vivo* sensing

[H3] Glucose sensing. A particular SERS sensing application that has been studied extensively for *in vivo* analysis is the quantification of glucose in blood. Pioneering studies focussed on developing SERS substrates suitable for *ex vivo* analyses, after which the materials were adapted to *in vivo* environments. SERS is a promising analytical technique for development of a continuous glucose monitoring device for improved care in diabetic patients. The state-of-the-art for glucose monitoring in diabetics has not advanced far from the first electrochemical sensor, the Ames Reflectance Meter,¹³⁶ which was first used in hospitals in the 1970s, and in homes in the 1980s.¹³⁷ This method uses glucose oxidase (GOx) to convert glucose to its corresponding lactone, with concomitant reduction of O₂ to H₂O₂. This ‘gold standard’ method is not ideal in that it requires blood to be drawn and it does not allow continuous monitoring, such that instances when blood glucose concentrations

are potentially dangerous may be missed. Continuous blood glucose monitoring can help minimize the long-term effects of hyperglycaemia and avoid hypoglycaemia by allowing more accurate control and administration of insulin. Recently, monitors have become available that address present shortcomings. One such device is FreeStyle Libre, which allows glucose measurements, acquired using an implanted needle patch, to be recorded more rapidly using a wireless scanning device.¹³⁸ Commercial devices enabling continuous glucose monitoring are also emerging, including a fluorescence-based detector developed by Dexcom.¹³⁹ Further optimization of continuous glucose monitors are necessary to improve the health of diabetic patients by providing a complete picture of fluctuating blood glucose levels. Ultimately, this could pave the way for using an artificial pancreas to combat diabetes by allowing feedback control for optimal operation.

When optimized, SERS has shown potential for overcoming many of the downfalls of other techniques. Early studies focused on developing a SERS substrate that would effectively and accurately detect and monitor glucose in real time in a minimally invasive fashion. One method uses Ag film over nanosphere (AgFON) and Au film over nanosphere (AuFON) substrates, which are to be implanted *in vivo*.⁷² (FIG. 4) SERS detection of the analyte requires it to be within a few nanometers of the substrate, which must be functionalised in order to more strongly and selectively bind glucose. Functionalization can involve the growth of a self-assembled monolayer (SAM) on the FON surface, which can now readily adsorb glucose such that it is in close proximity to the signal-enhancing metal. 1-Decanethiol (DT) afforded effective glucose-binding monolayers,¹⁴⁰ but its hydrophobicity was not amenable to an aqueous *in vivo* environment. Relative to DT SAMs, those based on (1-mercaptopundeca-11-yl)tri(ethylene glycol) showed increased stability (up to 10 days),⁷² reversibility, selectivity and biocompatibility.⁷⁵ These SAMs are not easily prepared, and a good practical alternative was found in monolayers comprising DT and mercaptohexanol (MH), which were used for *in vivo* measurements after establishing the real-time quantitative glucose monitoring capabilities for this SAM-FON *ex vivo* (FIG. 4a)¹⁴¹. The year 2006 saw the first use of this SAM-AgFON SERS sensor for glucose monitoring *in vivo*²⁹, incorporating an optical window into a live mouse to allow data collection. In 2010 came the first transcutaneous measurement using SESORS with the SAM-AgFON probe in a live rat⁴⁸ (FIG. 4b). This approach is superior in that a window is not required because the SERS sensor is implanted subcutaneously into the rat. SESORS-based measurements can now monitor glucose *in vivo* for more than than 17 days. More recently, the DT/MH system has been replaced with one based on a thiol-containing bis(boronic acid) receptor, which rapidly and preferentially binds glucose over other sugars⁵⁰. The resulting Raman data could be interpreted using multivariate statistical analysis to distinguish normal, hypoglycemic and hyperglycemic responses. This development takes *in vivo* SERS closer to the clinic, and is superior to earlier SERS technologies that already satisfy the hypoglycemic detection limits of the International Organisation Standard. Finally, an alternative SERS-based approach for glucose sensing involves quantifying GOx by interrogating its Raman-active flavin adenine dinucleotide¹⁴². Indeed, GOx bound to the surface of AgNPs gives a strong SERS signal, which is attenuated when glucose competes with the AgNP surface for GOx binding. This was the first report using SERS detection of GOx to measure glucose concentration, with the strong SERS enhancement allowing good sensitivity, and the use of an enzyme ensuring specificity towards glucose.

[H3] *Cancer detection.* SERS-based monitoring is very much amenable to the diagnosis of diseases, most notably cancer. Increasingly accurate and available techniques for cancer detection will ultimately lead to earlier diagnosis and increased survival rates. State-of-the-art clinical cancer diagnostics involve a trained pathologist examining a tissue biopsy sample and providing a diagnosis (histopathology).⁵ The procedure is inherently subjective and inevitably results in some incorrect diagnoses. Further, removing tissue from a patient during a biopsy and preparing it for analysis is time consuming and costly. Significant efforts have been made to develop infrared and Raman protocols to provide a more objective diagnosis according to the spectral signatures of disease markers present in the tissue section.⁵ However, these vibrational spectroscopic techniques have yet to be optimised for a clinical setting or prove superior to histopathology, and do not remove the need for cumbersome sample preparation.

Studies making use of SERS for *in vivo* cancer diagnosis could be the beginning of a push that may eventually allow *in vivo* detection without the need to remove and prepare biopsy tissue samples. This goal motivated the design of a SERS probe consisting of Au NPs decorated with diethylthiatricarbocyanine (a Raman reporter), and surrounded by a protective PEG layer. The surface of each particle is functionalized with single-chain variable fragment antibodies, moieties that selectively bind the EGFR, a protein overexpressed in many cancers¹¹⁸. These SERS probes, relative to fluorescent quantum dots, are more than 200× brighter, and exhibit SERS bands that are sharper and more distinguishable than the emission from the quantum dots. In a mouse, the Au NP-based probes selectively localize in tumour sites, which can then be visualized even when 1–2 cm from the skin surface.

The sensitivity of the above analyses has also been seen in related multiplexing experiments, and the sharp SERS peaks of four different probes have been resolved *in vivo*¹²². This work also included mapping experiments, in which the nanoprobe preferentially accumulate in a mouse liver, such that this region can be imaged *in vivo*. Likewise, three different SERS probes have been designed to actively target the EGFR, CD44 and TGF beta receptor II breast cancer biomarkers, enabling *in vivo* multiplexed detection in a mouse xenograft tumour⁵². Although SERS probes enable analyses with high sensitivity, ongoing efforts towards improving this are necessary because when *in vivo*, the Raman intensity is greatly attenuated as it travels through tissue, which can scatter a lot of light, particularly at long path lengths. As was presented earlier, efforts to address this involve designing Raman reporters optimized for NIR wavelengths, energies that are less well scattered by tissue. In this regard, crystal-violet-derived reporters can be functionalized with lipoic acid (LA), the disulfide group of which allows attachment to Au NPs¹⁴³. The resulting probes enable *in vivo* detection of EGFR and HER2 proteins, with more recent work with NIR-SERS reporters now allowing for multiplex detection of these biomarkers (FIG. 5).¹⁴⁴

There has been an increasing number of studies that not only focus on tracking SERS probes for *in vivo* cancer detection, but also address the imaging of tumours *in vivo*. We are of the opinion that the major advantage of SERS for *in vivo* detection does not lie in imaging, but rather its amenability to detect a real-time ‘yes or no’ response in a sensitive manner. The ability to rapidly image tumours could further improve this technology, perhaps most notably by allowing exact tumour margins to be visualized for resection. The major drawback of SERS imaging has been the time required for image acquisition, such that real-time analysis during surgery is not within our present capabilities. This is in part addressable by using wide-field imaging to enable rapid image acquisition, as has been used to image targeted SERS nanoprobe *in vitro*, *ex vivo*, and *in vivo*¹⁴⁵. Thus, multiple SERS nanoprobe, topically applied to tumour regions, could be located *in vivo*. This work made use of two EGFR-targeting probes as well as a non-targeting probe, the latter enabling non-specific binding to be accounted for to improve image contrast. This SERS method thus enables quantitative background correction, something not possible with fluorescence methods. As mentioned above, Raman has allowed for biomolecule detection down to 100 aM by making use of ultra-bright chalcogenopyrrium dyes that absorb in the NIR¹⁰⁶. Probes decorated with these dyes gave three times brighter EGFR imaging than those featuring the typical cyanine dye IR792 when intravenously injected in A431 xenograft nude mice (FIG. 5d,e). More recently, the benefits of topical probe dosage and acquisition of SERS background from non-targeted probes have been combined in a technique dubbed “topically applied surface-enhanced resonance Raman ratiometric spectroscopy (TAS3RS)”⁴⁹. Here, the NPs were administered intraperitoneally, in contrast to many other *in vivo* SERS studies that involve intravenous injection. We reiterate that the latter dosage method results in substantial probe concentrations in the liver and spleen, such that uptake into the regions of interest — tumour sites — is low. In addition, intraperitoneal administration avoids toxicity problems that can arise when NPs enter the systemic bloodstream. Therefore, although the progression of SERS into the clinic has been slowed by concerns over nanoparticle toxicity and biodistribution, these recent studies are beginning to surmount these barriers using alternative experimental design.

[H3] *Intraoperative guidance.* In order to ensure complete removal of tumours, it is extremely beneficial to perform selective imaging while surgery is being undertaken. SERS has shown promise

for intraoperative guidance because it is relatively fast, sensitive, and affords the possibility of obtaining fingerprint spectra with high specificity. Towards this, a dual-probe approach has been used whereby tissues from mouse tumours were incubated with two types of SERS-active NP, one featuring a EGFR-specific antibody and one with no targeting moiety. EGFR concentrations in fresh tissue samples can thus be measured by subtracting the background signals obtained¹⁴⁶. A single excitation wavelength was used to obtain distinct spectra from the two different probes, and it seems that the method will be extendable to include additional probes targeting different cancer markers, enabling significantly more accurate tumour detection. The method was later used to quantitatively phenotype tissue surfaces and could potentially lead to intraoperative detection of residual tumours in less than 15 minutes.⁵⁴

Earlier in this Review, we described a dual probe that could be interrogated using PA and SERS analysis. Building on this, a triple modality NP has been developed that allows simultaneous magnetic resonance imaging (MRI), PA and Raman imaging (MPR)¹⁴⁷. This MPR method combines the advantages of each technique to meet the needs for surgical resection of brain tumour patients. Each probe consists of a 60 nm AuNP functionalized with the Raman reporter 1,2-bis(4-pyridyl)ethylene, which is further protected by a 30 nm SiO₂ coating and a layer containing Gd(III) complexes, the paramagnetism of which ($S = 7/2$) provides good MRI contrast (FIG. 6a). The particles were visualized by consecutive magnetic resonance, PA and Raman imaging analyses, with detection limits of 4.88 pM for MRI, 1.22 pM for PA and 610 fM for Raman imaging. In live mice, the probes gave less sensitive magnetic resonance and PA responses due to the background signals from tissue. However, Raman imaging suffered negligible interference from tissue signals, and the particles could be clearly observed down to 50 pM, the lowest concentration investigated *in vivo*. Following injection of the particles into mice having brain tumours, each of the three methods allowed visualization of the cancerous regions, even through the intact skin and skull (FIG. 6b). By imaging the interface between the tumour and the healthy tissue, a strong Raman signal could be observed from within the tumour but not from surrounding areas (FIG. 6c). This is because the MPR particles accumulate in the tumour region but are too large to cross the blood-brain barrier, and therefore do not accumulate in healthy brain tissue. Due to the sensitivity of the SERS method, Raman signals could also be obtained from tumour protrusions and microscopic tumour foci. Indeed, Raman imaging has been employed to guide tumour resection, and images obtained at each stage correlate well with photographs. Additionally, when the tumour appeared to be completely removed by visual inspection, Raman signals could still be observed from small areas, regions that were later found to be cancerous extensions into the surrounding tissues. Although they were not visually apparent, they were detectable by Raman imaging due to the selective accumulation of MPR particles in the cancerous regions. These particles also allowed the same probe to be observed before and during surgery, enabling brain tumour resection with improved accuracy. The sensitivity of Raman imaging was important in allowing detection of microscopic tumour deposits not otherwise visible, thus allowing complete removal of cancerous tissues. This was due to the strong, unique spectra obtained from SERS imaging and the lack of background signals, which are apparent in other imaging techniques, in which fluorescence from surrounding tissues can interfere with the output signal.

[H3] Drug delivery and photothermal therapy. Au NPs have unique optical properties, biocompatibility and ease of functionalization that makes them particularly suitable in drug delivery,^{95,99,148} controlled DNA release,¹⁴⁹⁻¹⁵¹ active tumour targeting,^{52,118,144} photodynamic therapy (PDT)^{94,152} and PTT.^{92,98,100,153} Additionally, the use of NPs in these applications provides enhanced signals in Raman imaging and allows the processes to be monitored using SERS. Relative to healthy tissue, tumours are more permeable to NPs and retain them for longer, such that NP-based imaging agents or drugs can reach the tumour site and have the desired effect specifically in the target region. One can prepare Au nanospheres that bind the anticancer drug doxorubicin (DOX) *via* an acid-sensitive linkage, such that the drug can be delivered to lysosomes in single cells¹⁵⁴. When in the lysosomes, the acidic environment induces DOX release from the NPs, such that SERS is attenuated and fluorescence increases because DOX is further from the quenching NP surface. By monitoring the rise of one signal and fall of the other, one can track drug release using both fluorescence and SERS.

Au nanorods (AuNRs) coated with PEG groups and a DTTC reporter have been found to passively accumulate in tumours, allowing photothermal heating of only the tumour region. SERS from the reporter could be obtained from the tumour *in vivo*, such that the AuNRs could potentially be used as a hyperthermia agent in cancer treatment, with effective monitoring by SERS⁹⁵. They also demonstrated the thermally controlled release of DOX using temperature-sensitive lipid components, and found that the photothermal effect from the AuNRs significantly increased the toxicity of DOX to the cancer cells, and improved the accumulation of the drug in tumours *in vivo* (FIG. 7a–c). Two separate NP formulations were used to demonstrate the hyperthermia effect and drug release capabilities, with fluorescence imaging being employed for the latter⁹⁵. However, SERS could also be utilized here by replacing the fluorophore with a Raman reporter. Later work showed that AuNRs functionalized with various Raman reporters, on 785 nm laser excitation, gave significant, distinguishable SERS that could be detected *in vivo*. The same tagged AuNRs could be heated rapidly to 70 °C *in vivo*, following irradiation at 810 nm, with no loss in SERS signal intensity.⁹² In an interesting and novel development, use has been made of a dye-free approach, in which AuNRs were functionalised only with a conducting polymer, which serves both as a biocompatible coating and a NIR Raman reporter¹¹³. These nanoprobes showed excellent biocompatibility and have been applied to SERS imaging and PTT of tumours *in vitro* and *in vivo*. More recently developed probes include Au nanostars (AuNSs), which can be functionalized with the anticancer drug mitoxantrone (MTX). The distinct Raman spectrum of MTX, combined with the significant SERS enhancement from the nanostars, allows one to track delivery and release of MTX *in vivo* and in real-time using SERS⁹⁹. Related work has illustrated the value of AuNSs in SERS imaging as well as PTT *in vivo* (FIG. 7d–f)¹⁰⁰. AgNPs coated with AuNSs are biocompatible, and on functionalization with DTTC, give rise to intense SERS spectra *in vitro* and *in vivo*. These Ag@Au-DTTC materials are further useful in that the AuNSs are extremely efficient for PTT⁹⁸. AuNSs can be decorated with Gd(III) complexes such that SERS and MRI can be combined in sensitive and high resolution imaging to guide PTT and monitor response¹⁵⁵. Here, the AuNSs provide significant enhancement of SERS signals and photothermal heating, while Gd(III) acts as a magnetic resonance imaging contrast agent. Irradiating into the 800 nm absorption band of the magnetic Au nanostar-based nanocomposites (MAuSNs) gave rise to excellent photothermal heating, and the probes are relatively stable once coated in an organosilica layer. Even under laser irradiation, the MAuSNs showed negligible toxicity towards two healthy cell lines across a range of particle concentrations. *In vivo* SERS with irradiation at 785 nm allows one to pinpoint the Raman reporter in different sites within a tumour, and no signal is observed from other skin areas or from a tumour injected with saline in place of the NPs. SERS imaging of NP distribution within the tumour is also possible, an analysis that may well help guide therapy. However, as previously mentioned, we believe that the real advantages of *in vivo* SERS come from its sensitivity, specificity and multiplexing capabilities. Thus, a ‘yes or no’ signal can be obtained specifically from multiple targets in a desired area with high sensitivity and resolution and little interference from surrounding tissues. Nonetheless, the imaging aspects are useful here, particularly when combined with MRI, to confirm the accumulation of the NPs in the tumour prior to PTT tests. Cancerous mice injected with MAuSNs, on exposure to 785 nm laser irradiation, experienced significant heating around their tumours, with negligible heating observed when saline solution was injected as a control. The role of PTT is undeniable — MAuSN treatment and irradiation completely killed the tumours after two days, while cancerous regions in the control groups underwent rapid growth. The *in vivo* toxicity of MAuSNs was also investigated, and they inflict no significant damage to tissues, nor do they change blood properties tested, indicating that they should be safe for clinical application.

The many examples above illustrate that the properties of Au NPs — particularly nanorods and nanostars — are well suited to imaging and therapeutic applications. SERS has significant potential as the detection technique in these cases due to its sensitivity, unique fingerprint signals and the fact that enhanced spectra can be obtained specifically from areas where NPs accumulate. Additionally, the biocompatibilities of many of these particles indicate that they are safe for *in vivo* application. Although more thorough investigation must precede translation to the clinic, the use of these NPs in conjunction with SERS, holds substantial promise in biosensing. We envisage this will attract a great deal of focus in the coming years.

[H1] Conclusions

Significant progress has been made in developing nanosensors for the application of SERS *in vivo*. Suitable metal substrates with highly tuneable optical properties now allow high SERS signal enhancements at laser wavelengths that are safe to the body and do not give rise to interference from tissues and biomolecules. SERS reporters exist that are not only sensitive at long wavelengths, but also allow for additional advantages such as multiplexing. The biocompatibility of nanoprobe has also been improved by careful selection of the substrate, and application of protective coatings. Yet, cytotoxicity remains a concern that holds back clinical application of SERS, and extensive research will be necessary to determine the most biocompatible and stable nanoprobe for use in humans. Many recent studies have indicated that the topical application of nanoprobe (as opposed to intravenous injection) could be particularly successful in helping SERS detection into the clinic. Topical application has already been shown to result in decreased toxicity and more effective targeting because nanoprobe do not pass into the systemic bloodstream or accumulate in the liver or spleen. Nanoprobe can be administered topically when tissues are accessible *via* endoscopic probe, a procedure that appears amenable to human use.

In terms of instrumentation, new designs can be portable and penetrate tissue more deeply, which is of particular benefit to *in vivo* applications. In many applications, particularly glucose monitoring, clinical use will demand instrumentation to be yet more straightforward and user-friendly than the rather specialised equipment in use at the time of writing this Review. A number of Raman accessories suitable for insertion into standard endoscopic probe have been developed, including a device capable of rapid 2D or 3D imaging easily interpretable by a physician.¹³¹ The convenience afforded by these recent studies, in our opinion, will be key in moving SERS into the clinic. Incredible developments have been made in regard to SERS applications in glucose sensing and cancer detection. The technique offers the requisite sensitivity, specificity, throughput and non-invasiveness that will no doubt attract further interest and continued research in biosensing and biomedical contexts. Additionally, SERS imaging has shown potential in theranostics, for intraoperative guidance, and for the detection and monitoring of drug treatment and therapy. Useful in isolation, SERS can also be combined with other methods such as fluorescence, MRI and photoacoustic imaging. Such multimodal analyses offer improved sensitivity, specificity and accuracy in the detection and diagnosis of disease, as well as allowing for greater treatment efficacy. With all of this in mind, we foresee that SERS will continue to be explored extensively for *in vivo* applications, which may well lead to SERS eventually finding clinical use for efficient diagnostics and therapy guidance. Since the first detection of biomolecules using SERS almost 30 years ago, the technique has shown enormous promise in biomedical applications. A decade has passed since the first application of SERS *in vivo*. This Review has largely discussed the development and application of SERS sensors, work that mostly involves animal models. We predict that research in the next decade will aim toward progression into *in vivo* detection in humans and the use of SERS in a clinical environment.

[H1] References

- 1 Raman, C. V. & Krishnan, K. S. A new type of secondary radiation. *Nature* **121**, 501–502 (1928).
- 2 Raman, C. V. A new radiation. *Indian J. Phys.* **2**, 387–398 (1928).
- 3 Diem, M., Romeo, M., Boydston-White, S., Miljković, M. & Matthäus, C. A decade of vibrational micro-spectroscopy of human cells and tissue (1994–2004). *Analyst* **129**, 880–885 (2004).
- 4 Kong, K., Kendall, C., Stone, N. & Notingher, I. Raman spectroscopy for medical diagnostics — from in-vitro biofluid assays to in-vivo cancer detection. *Adv. Drug Deliv. Rev.* **89**, 121–134 (2015).
- 5 Byrne, H. J. *et al.* Spectropathology for the next generation: quo vadis? *Analyst* **140**, 2066–2073 (2015).
- 6 Stone, N., Kendall, C., Smith, J., Crow, P. & Barr, H. Raman spectroscopy for identification of epithelial cancers. *Faraday Discuss.* **126**, 141–157 (2004).

- 7 Jamieson, L. E. & Byrne, H. J. Vibrational spectroscopy as a tool for studying drug–cell interaction: Could high throughput vibrational spectroscopic screening improve drug development? *Vib. Spectrosc.* (doi: <http://dx.doi.org/10.1016/j.vibspec.2016.09.003>).
- 8 Farhane, Z., Bonnier, F., Casey, A. & Byrne, H. J. Raman micro spectroscopy for *in vitro* drug screening: subcellular localisation and interactions of doxorubicin. *Analyst* **140**, 4212–4223 (2015).
- 9 Matthäus, C., Kale, A., Chernenko, T., Torchilin, V. & Diem, M. New ways of imaging uptake and intracellular fate of liposomal drug carrier systems inside individual cells, based on Raman microscopy. *Mol. Pharm.* **5**, 287–293 (2008).
- 10 Atkins, P., de Paula, J. & Friedman, R. *Physical chemistry: quanta, matter, and change.* (OUP Oxford, 2013).
- 11 Fleischmann, M., Hendra, P. J. & McQuillan, A. J. Raman spectra of pyridine adsorbed at a silver electrode. *Chem. Phys. Lett.* **26**, 163–166 (1974).
- 12 Bergman, I. *et al.* General discussion. *Faraday Discuss. Chem. Soc.* **56**, 152–170 (1973).
- 13 Jeanmaire, D. L. & Van Duyne, R. P. Surface Raman spectroelectrochemistry: Part I. Heterocyclic, aromatic, and aliphatic amines adsorbed on the anodized silver electrode. *J. Electroanal. Chem. Interfacial Electrochem.* **84**, 1–20 (1977).
- 14 Yang, S., Dai, X., Stogin, B. B. & Wong, T.-S. Ultrasensitive surface-enhanced Raman scattering detection in common fluids. *Proc. Natl Acad. Sci. U. S. A.* **113**, 268–273 (2016).
- 15 Kneipp, J., Kneipp, H. & Kneipp, K. SERS—a single-molecule and nanoscale tool for bioanalytics. *Chem. Soc. Rev.* **37**, 1052–1060 (2008).
- 16 Smith, E. & Dent, G. *Modern Raman spectroscopy: a practical approach.* (Wiley, 2013).
- 17 Campion, A. & Kambhampati, P. Surface-enhanced Raman scattering. *Chem. Soc. Rev.* **27**, 241–250 (1998).
- 18 Schlücker, S. Surface-enhanced Raman spectroscopy: concepts and chemical applications. *Angew. Chem. Int. Ed.* **53**, 4756–4795 (2014).
- 19 Stiles, P. L., Dieringer, J. A., Shah, N. C. & Van Duyne, R. R. Surface-enhanced Raman spectroscopy. *Annu. Rev. Anal. Chem.* **1**, 601–626 (2008).
- 20 Vo-Dinh, T., Hiromoto, M. Y. K., Begun, G. M. & Moody, R. L. Surface-enhanced Raman spectrometry for trace organic analysis. *Anal. Chem.* **56**, 1667–1670 (1984).
- 21 Rohr, T. E., Cotton, T., Fan, N. & Tarcha, P. J. Immunoassay employing surface-enhanced Raman spectroscopy. *Anal. Biochem.* **182**, 388–398 (1989).
- 22 Vo-Dinh, T., Houck, K. & Stokes, D. L. Surface-enhanced Raman gene probes. *Anal. Chem.* **66**, 3379–3383 (1994).
- 23 Graham, D., Mallinder, B. J. & Smith, W. E. Surface-enhanced resonance Raman scattering as a novel method of DNA discrimination. *Angew. Chem. Int. Ed.* **39**, 1061–1063 (2000).
- 24 Faulds, K., Jarvis, R., Smith, W. E., Graham, D. & Goodacre, R. Multiplexed detection of six labelled oligonucleotides using surface enhanced resonance Raman scattering (SERRS). *Analyst* **133**, 1505–1512 (2008).
- 25 Gracie, K. *et al.* Simultaneous detection and quantification of three bacterial meningitis pathogens by SERS. *Chem. Sci.* **5**, 1030–1040 (2014).
- 26 Song, J., Zhou, J. & Duan, H. Self-assembled plasmonic vesicles of SERS-encoded amphiphilic gold nanoparticles for cancer cell targeting and traceable intracellular drug delivery. *J. Am. Chem. Soc.* **134**, 13458–13469 (2012).
- 27 Nabiev, I. R., Morjani, H. & Manfait, M. Selective analysis of antitumor drug interaction with living cancer cells as probed by surface-enhanced Raman spectroscopy. *Eur. Biophys. J.* **19**, 311–316 (1991).
- 28 Schlücker, S. *et al.* Immuno-Raman microspectroscopy: *in situ* detection of antigens in tissue specimens by surface-enhanced Raman scattering. *J. Raman Spectrosc.* **37**, 719–721 (2006).
- 29 Stuart, D. A. *et al.* *In vivo* glucose measurement by surface-enhanced Raman spectroscopy. *Anal. Chem.* **78**, 7211–7215 (2006).
- This was the first example of SERS being used *in vivo*, with the specific application being for monitoring of glucose concentration in a live mouse using a SAM–AgFON SERS sensor and an optical window.**
- 30 White, P. L. *et al.* Evaluation of a commercially developed

- semiautomated PCR–surface-enhanced Raman scattering assay for diagnosis of invasive fungal disease. *J. Clin. Microbiol.* **52**, 3536–3543 (2014).
- 31 *Industry News: Renishaw Diagnostics Announces CE Marking of Rendx® Multiplex Assay System and Fungiplex Assay* <<http://www.selectscience.net/industry-news/renishaw-diagnostics-announces-ce-marking-of-rendx-multiplex-assay-system-and-fungiplex-assay/?artID=38483>> (2015).
- 32 Graham, D., Faulds, K., Smith, W. E. & Ricketts, A. Identification of nucleic acid sequences WO 2009/022125 A1 (2009).
- 33 Cai, W., Gao, T., Hong, H. & Sun, J. Applications of gold nanoparticles in cancer nanotechnology. *Nanotechnol. Sci. Appl.* **2008**, 10.2147/NSA.S3788 (2008).
- 34 Caspers, P. J., Lucassen, G. W. & Puppels, G. J. Combined *in vivo* confocal Raman spectroscopy and confocal microscopy of human skin. *Biophys. J.* **85**, 572–580 (2003).
- 35 Boncheva, M., de Sterke, J., Caspers, P. J. & Puppels, G. J. Depth profiling of *Stratum corneum* hydration *in vivo*: a comparison between conductance and confocal Raman spectroscopic measurements. *Exp. Dermatol.* **18**, 870–876 (2009).
- 36 Mahadevan-Jansen, A., Mitchell, M. F., Ramanujam, N., Utzinger, U. & Richards-Kortum, R. Development of a fiber optic probe to measure NIR Raman spectra of cervical tissue *in vivo*. *Photochem. Photobiol.* **68**, 427–431 (1998).
- 37 Draga, R. O. *et al.* *In vivo* bladder cancer diagnosis by high-volume Raman spectroscopy. *Anal. Chem.* **82**, 5993–5999 (2010).
- 38 Shim, M. G., Song, L. M., Marcon, N. E. & Wilson, B. C. *In vivo* near-infrared Raman spectroscopy: demonstration of feasibility during clinical gastrointestinal endoscopy. *Photochem. Photobiol.* **72**, 146–150 (2000).
- 39 Haka, A. S. *et al.* *In vivo* margin assessment during partial mastectomy breast surgery using Raman spectroscopy. *Cancer Res.* **66**, 3317–3322 (2006).
- 40 Jermyn, M. *et al.* Intraoperative brain cancer detection with Raman spectroscopy in humans. *Sci. Transl. Med.* **7**, 274ra219 (2015).
- 41 *Laser detects brain tumour cells during surgery*, <<http://www.bbc.co.uk/news/health-34041863>> (2015).
- 42 *Verisante Aura*, <http://www.verisante.com/aura/medical_professional/> (Accessed 2017).
- 43 *UK hospital to trial Raman probe for brain tumors*, <<http://optics.org/news/6/1/18>> (2015).
- 44 Evans, C. L. *et al.* Chemical imaging of tissue *in vivo* with video-rate coherent anti-Stokes Raman scattering microscopy. *Proc. Natl Acad. Sci. U. S. A.* **102**, 16807–16812 (2005).
- 45 Fu, Y., Huff, T. B., Wang, H. W., Wang, H. & Cheng, J. X. *Ex vivo* and *in vivo* imaging of myelin fibers in mouse brain by coherent anti-Stokes Raman scattering microscopy. *Opt Express* **16**, 19396–19409 (2008).
- 46 Ji, M. *et al.* Rapid, label-free detection of brain tumors with stimulated Raman scattering microscopy. *Sci. Transl. Med.* **5**, 201ra119 (2013).
- 47 Saar, B. G. *et al.* Video-rate molecular imaging *in vivo* with stimulated Raman scattering. *Science* **330**, 1368–1370 (2010).
- 48 Yuen, J. M., Shah, N. C., Walsh, J. T., Glucksberg, M. R. & Van Duyne, R. P. Transcutaneous glucose sensing by surface-enhanced spatially offset Raman spectroscopy in a rat model. *Anal. Chem.* **82**, 8382–8385 (2010).
- 49 Oseledchyk, A., Andreou, C., Wall, M. A. & Kircher, M. F. Folate-targeted surface-enhanced resonance Raman scattering nanoprobe ratiometry for detection of microscopic ovarian cancer. *ACS Nano* **11**, 1488–1497 (2017).
- 50 Sharma, B. *et al.* Bisboronic acids for selective, physiologically relevant direct glucose sensing with surface-enhanced Raman spectroscopy. *J. Am. Chem. Soc.* **138**, 13952–13959 (2016).
- 51 Ma, K. *et al.* *In vivo*, transcutaneous glucose sensing using surface-enhanced spatially offset Raman spectroscopy: multiple rats, improved hypoglycemic accuracy, low incident power, and continuous monitoring for greater than 17 days. *Anal. Chem.* **83**, 9146–9152 (2011).
- 52 Dinish, U. S., Balasundaram, G., Chang, Y.-T. & Olivo, M. Actively targeted *in vivo* multiplex detection of intrinsic cancer biomarkers using biocompatible SERS nanotags. *Sci. Rep.* **4**, 4075 (2014).

53 Samanta, A. *et al.* Ultrasensitive near-infrared Raman reporters for SERS-based *in vivo* cancer detection. *Angew. Chem. Int. Ed.* **50**, 6089–6092 (2011).

In this study a library of tricarbocyanine reporters, optimised for NIR excitation, were synthesised and screened and CyNAMLA-381 was subsequently used for sensitive and specific tumour detection.

- 54 Wang, Y. *et al.* Quantitative molecular phenotyping with topically applied SERS nanoparticles for intraoperative guidance of breast cancer lumpectomy. *Sci. Rep.* **6**, 21242 (2016).
- 55 Tian, F. *et al.* Gold nanostars for efficient *in vitro* and *in vivo* real-time SERS detection and drug delivery *via* plasmonic-tunable Raman/FTIR imaging. *Biomaterials* **106**, 87–97 (2016).
- 56 Papadopoulou, E. & Bell, S. E. J. Label-free detection of single-base mismatches in DNA by surface-enhanced Raman spectroscopy. *Angew. Chem. Int. Ed.* **50**, 9058–9061 (2011).
- 57 Pavel, I. *et al.* Label-free SERS detection of small proteins modified to act as bifunctional linkers. *J. Phys. Chem. C* **112**, 4880–4883 (2008).
- 58 Graham, D. *et al.* Synthesis of novel monoazo benzotriazole dyes specifically for surface enhanced resonance Raman scattering. *Chem. Commun.*, 1187–1188 (1998).
- 59 Schütz, M., Müller, C. I., Salehi, M., Lambert, C. & Schlücker, S. Design and synthesis of Raman reporter molecules for tissue imaging by immuno-SERS microscopy. *J. Biophotonics* **4**, 453–463 (2011).
- 60 Faulds, K., Smith, W. E. & Graham, D. DNA detection by surface enhanced resonance Raman scattering (SERRS). *Analyst* **130**, 1125–1131 (2005).
- 61 Drescher, D. & Kneipp, J. Nanomaterials in complex biological systems: insights from Raman spectroscopy. *Chem. Soc. Rev.* **41**, 5780–5799 (2012).
- 62 Taylor, J., Huefner, A., Li, L., Wingfield, J. & Mahajan, S. Nanoparticles and intracellular applications of surface-enhanced Raman spectroscopy. *Analyst* **141**, 5037–5055 (2016).
- 63 Alkilany, A. M. & Murphy, C. J. Toxicity and cellular uptake of gold nanoparticles: what we have learned so far? *J. Nanopart. Res.* **12**, 2313–2333 (2010).
- 64 Sakhtianchi, R. *et al.* Exocytosis of nanoparticles from cells: role in cellular retention and toxicity. *Adv. Colloid Interface Sci.* **201**, 18–29 (2013).
- 65 Dykman, L. A. & Khlebtsov, N. G. Uptake of engineered gold nanoparticles into mammalian cells. *Chem. Rev.* **114**, 1258–1288 (2014).
- 66 Zhang, X.-D. *et al.* Size-dependent *in vivo* toxicity of PEG-coated gold nanoparticles. *Int. J. Nanomed.* **6**, 2071–2081 (2011).
- 67 Bhamidipati, M. & Fabris, L. Multiparametric assessment of gold nanoparticle cytotoxicity in cancerous and healthy cells: the role of size, shape, and surface chemistry. *Bioconj. Chem.* **28**, 449–460 (2017).
- 68 Schlinkert, P. *et al.* The oxidative potential of differently charged silver and gold nanoparticles on three human lung epithelial cell types. *J. Nanobiotechnol.* **13**, 18 (2015).
- 69 Falagan-Lotsch, P., Grzincic, E. M. & Murphy, C. J. One low-dose exposure of gold nanoparticles induces long-term changes in human cells. *Proc. Natl Acad. Sci. U. S. A.* **113**, 13318–13323 (2016).
- 70 Albanese, A. & Chan, W. C. W. Effect of gold nanoparticle aggregation on cell uptake and toxicity. *Acs Nano* **5**, 5478–5489 (2011).
- 71 Weissleder, R. A clearer vision for *in vivo* imaging. *Nat. Biotechnol.* **19**, 316–317 (2001).
- 72 Stuart, D. A. *et al.* Glucose sensing using near-infrared surface-enhanced Raman spectroscopy: gold surfaces, 10-day stability, and improved accuracy. *Anal. Chem.* **77**, 4013–4019 (2005).
- 73 Mahajan, S. *et al.* Tuning plasmons on nano-structured substrates for NIR-SERS. *Phys. Chem. Chem. Phys.* **9**, 104–109 (2007).
- 74 Greeneltch, N. G. *et al.* Near-infrared surface-enhanced Raman spectroscopy (NIR-SERS) for the identification of eosin Y: theoretical calculations and evaluation of two different nanoplasmonic substrates. *J. Phys. Chem. A* **116**, 11863–11869 (2012).
- 75 Yonzon, C. R., Haynes, C. L., Zhang, X., Walsh, J. T. & Van Duyne, R. P. A glucose biosensor based on surface-enhanced Raman scattering: improved partition layer, temporal stability, reversibility, and resistance to serum protein interference. *Anal. Chem.* **76**, 78–85 (2004).

- 76 Asharani, P. V., Yi Lian, W., Zhiyuan, G. & Suresh, V. Toxicity of silver nanoparticles in zebrafish models. *Nanotechnology* **19**, 255102 (2008).
- 77 Asharani, P. V., Mun, G. L. K., Hande, M. P. & Valiyaveetil, S. Cytotoxicity and genotoxicity of silver nanoparticles in human cells. *ACS Nano* **3**, 279–290 (2009).
- 78 Liu, W. *et al.* Impact of silver nanoparticles on human cells: effect of particle size. *Nanotoxicology* **4**, 319–330 (2010).
- 79 Shukla, R. *et al.* Biocompatibility of gold nanoparticles and their endocytotic fate inside the cellular compartment: a microscopic overview. *Langmuir* **21**, 10644–10654 (2005).
- 80 Averitt, R. D., Sarkar, D. & Halas, N. J. Plasmon resonance shifts of Au-coated Au₂S nanoshells: insight into multicomponent nanoparticle growth. *Phys. Rev. Lett.* **78**, 4217–4220 (1997).
- 81 Oldenburg, S. J., Averitt, R. D., Westcott, S. L. & Halas, N. J. Nanoengineering of optical resonances. *Chem. Phys. Lett.* **288**, 243–247 (1998).
- 82 Oldenburg, S. J., Westcott, S. L., Averitt, R. D. & Halas, N. J. Surface enhanced Raman scattering in the near infrared using metal nanoshell substrates. *J. Chem. Phys.* **111**, 4729–4735 (1999).
- 83 Küstner, B. *et al.* SERS Labels for Red Laser Excitation: Silica-Encapsulated SAMs on Tunable Gold/Silver Nanoshells. *Angew. Chem. Int. Ed.* **48**, 1950–1953 (2009).
- 84 Kang, H. *et al.* Near-Infrared SERS Nanoprobes with plasmonic Au/Ag hollow-shell assemblies for *in vivo* multiplex detection. *Adv. Funct. Mater.* **23**, 3719–3727 (2013).
- 85 Sun, Y., Mayers, B. T. & Xia, Y. Template-engaged replacement reaction: a one-step approach to the large-scale synthesis of metal nanostructures with hollow interiors. *Nano Lett.* **2**, 481–485 (2002).
- 86 Liang, H. P., Wan, L. J., Bai, C. L. & Jiang, L. Gold hollow nanospheres: tunable surface plasmon resonance controlled by interior-cavity sizes. *J. Phys. Chem. B* **109**, 7795–7800 (2005).
- 87 Schwartzberg, A. M., Olson, T. Y., Talley, C. E. & Zhang, J. Z. Synthesis, characterization, and tunable optical properties of hollow gold nanospheres. *J. Phys. Chem. B* **110**, 19935–19944 (2006).
- 88 Xie, H. N., Larmour, I. A., Smith, W. E., Faulds, K. & Graham, D. Surface-enhanced Raman scattering investigation of hollow gold nanospheres. *J. Phys. Chem. C* **116**, 8338–8342 (2012).
- 89 Xie, H. N. *et al.* Synthesis and NIR optical properties of hollow gold nanospheres with LSPR greater than one micrometer. *Nanoscale* **5**, 765–771 (2013).
- 90 Kearns, H., Shand, N. C., Smith, W. E., Faulds, K. & Graham, D. 1064 nm SERS of NIR active hollow gold nanotags. *Phys. Chem. Chem. Phys.* **17**, 1980–1986 (2015).
- 91 Adams, S. & Zhang, J. Z. Unique optical properties and applications of hollow gold nanospheres (HGNs). *Coord. Chem. Rev.* **320**, 18–37 (2016).
- 92 von Maltzahn, G. *et al.* SERS-coded gold nanorods as a multifunctional platform for densely multiplexed near-infrared imaging and photothermal heating. *Adv. Mater.* **21**, 3175–3180 (2009).
- 93 Wu, L. *et al.* A SERS-based immunoassay with highly increased sensitivity using gold/silver core-shell nanorods. *Biosens. Bioelectron.* **38**, 94–99 (2012).
- 94 Zhang, Y., Qian, J., Wang, D., Wang, Y. & He, S. Multifunctional gold nanorods with ultrahigh stability and tunability for *in vivo* fluorescence imaging, SERS detection, and photodynamic therapy. *Angew. Chem. Int. Ed.* **52**, 1148–1151 (2013).
- 95 Park, J.-H. *et al.* Cooperative nanoparticles for tumor detection and photothermally triggered drug delivery. *Adv. Mater.* **22**, 880–885 (2010).
- This study demonstrated the use of GNRs for thermally controlled drug release, directly in tumour sites, with detection by SERS, signifying the potential of the technique for diagnostic and therapeutic applications.**
- 96 Harmsen, S. *et al.* Surface-enhanced resonance Raman scattering nanostars for high-precision cancer imaging. *Sci. Transl. Med.* **7**, 271ra277 (2015).
- 97 Register, J. K. *et al.* *In vivo* detection of SERS-encoded plasmonic nanostars in human skin grafts and live animal models. *Anal. Bioanal. Chem.* **407**, 8215–8224 (2015).

- 98 Zeng, L. *et al.* Raman reporter-coupled Ag_{core}@Au_{shell} nanostars for *in vivo* improved surface enhanced Raman scattering imaging and near-infrared-triggered photothermal therapy in breast cancers. *ACS Appl. Mater. Interfaces* **7**, 16781–16791 (2015).
- 99 Tian, F. *et al.* Gold nanostars for efficient *in vitro* and *in vivo* real-time SERS detection and drug delivery *via* plasmonic-tunable Raman/FTIR imaging. *Biomaterials* **106**, 87–97 (2016).
- 100 Liu, Y. *et al.* A plasmonic gold nanostar theranostic probe for *in vivo* tumor imaging and photothermal therapy. *Theranostics* **5**, 946–960 (2015).
- 101 Maiti, K. K. *et al.* Multiplex cancer cell detection by SERS nanotags with cyanine and triphenylmethine Raman reporters. *Chem. Commun.* **47**, 3514–3516 (2011).
- 102 Samanta, A., Das, R. K., Park, S. J., Maiti, K. K. & Chang, Y. T. Multiplexing SERS nanotags for the imaging of differentiated mouse embryonic stem cells (mESC) and detection of teratoma *in vivo*. *Am. J. Nucl. Med. Mol. Imaging* **4**, 114–124 (2014).
- 103 Wustholz, K. L., Brosseau, C. L., Casadio, F. & Van Duyne, R. P. Surface-enhanced Raman spectroscopy of dyes: from single molecules to the artists' canvas. *Phys. Chem. Chem. Phys.* **11**, 7350–7359 (2009).
- 104 McAughtrie, S., Lau, K., Faulds, K. & Graham, D. 3D optical imaging of multiple SERS nanotags in cells. *Chem. Sci.* **4**, 3566–3572 (2013).
- 105 Bedics, M. A. *et al.* Extreme red shifted SERS nanotags. *Chem. Sci.* **6**, 2302–2306 (2015).
- 106 Harmsen, S. *et al.* Rational design of a chalcogenopyrylium-based surface-enhanced resonance Raman scattering nanoprobe with attomolar sensitivity. *Nat. Commun.* **6**, 9 (2015).
A group of NIR dyes were designed and used with Au NPs to yield biocompatible SERRS probes with exceptionally high sensitivity.
- 107 Kearns, H. *et al.* Sensitive SERS nanotags for use with 1550 nm (retina-safe) laser excitation. *Analyst* **141**, 5062–5065 (2016).
- 108 Dinish, U. S. *et al.* Single molecule with dual function on nanogold: biofunctionalized construct for *in vivo* photoacoustic imaging and SERS biosensing. *Adv. Funct. Mater.* **25**, 2316–2325 (2015).
- 109 McQueenie, R. *et al.* Detection of inflammation *in vivo* by surface-enhanced Raman scattering provides higher sensitivity than conventional fluorescence imaging. *Anal. Chem.* **84**, 5968–5975 (2012).
- 110 Wu, X., Chen, J., Wu, M. & Zhao, J. X. Aptamers: active targeting ligands for cancer diagnosis and therapy. *Theranostics* **5**, 322–344 (2015).
- 111 Zong, S. *et al.* A SERS and fluorescence dual mode cancer cell targeting probe based on silica coated Au@Ag core–shell nanorods. *Talanta* **97**, 368–375 (2012).
- 112 Iacono, P., Karabeber, H. & Kircher, M. F. A “schizophotonic” all-in-one nanoparticle coating for multiplexed SE(R)RS biomedical imaging. *Angew. Chem. Int. Ed.* **53**, 11756–11761 (2014).
- 113 Liu, Z. M. *et al.* Dye-free near-infrared surface-enhanced Raman scattering nanoprobe for bioimaging and high-performance photothermal cancer therapy. *Nanoscale* **7**, 6754–6761 (2015).
- 114 Jiang, C. H., Wang, Y., Wang, J. W., Song, W. & Lu, L. H. Achieving ultrasensitive *in vivo* detection of bone crack with polydopamine-capsulated surface-enhanced Raman nanoparticle. *Biomaterials* **114**, 54–61 (2017).
- 115 Kim, J. H. *et al.* Nanoparticle probes with surface enhanced Raman spectroscopic tags for cellular cancer targeting. *Anal. Chem.* **78**, 6967–6973 (2006).
- 116 Zhang, Z. *et al.* Mesoporous silica-coated gold nanorods as a light-mediated multifunctional theranostic platform for cancer treatment. *Adv. Mater.* **24**, 1418–1423 (2012).
- 117 Doering, W. E. & Nie, S. Spectroscopic tags using dye-embedded nanoparticles and surface-enhanced Raman scattering. *Anal. Chem.* **75**, 6171–6176 (2003).
- 118 Qian, X. *et al.* *In vivo* tumor targeting and spectroscopic detection with surface-enhanced Raman nanoparticle tags. *Nat. Biotechnol.* **26**, 83–90 (2008).
This study was the first application of a SERS probe for cancer detection *in vivo*, and used Au NPs functionalized with diethylthiatricarbocyanine, a protective PEG layer, and single-chain variable fragment antibodies, to selectively bind EGFR.

- 119 Jokerst, J. V., Lobovkina, T., Zare, R. N. & Gambhir, S. S. Nanoparticle PEGylation for imaging and therapy. *Nanomedicine* **6**, 715–728 (2011).
- 120 Potara, M., Baia, M., Farcau, C. & Astilean, S. Chitosan-coated anisotropic silver nanoparticles as a SERS substrate for single-molecule detection. *Nanotechnology* **23** (2012).
- 121 Potara, M. *et al.* Chitosan-coated triangular silver nanoparticles as a novel class of biocompatible, highly sensitive plasmonic platforms for intracellular SERS sensing and imaging. *Nanoscale* **5**, 6013–6022 (2013).
- 122 Keren, S. *et al.* Noninvasive molecular imaging of small living subjects using Raman spectroscopy. *Proc. Natl Acad. Sci. U. S. A.* **105**, 5844–5849 (2008).
- 123 Bohndiek, S. E. *et al.* A small animal Raman instrument for rapid, wide-area, spectroscopic imaging. *Proc. Natl Acad. Sci. U. S. A.* **110**, 12408–12413 (2013).
- 124 Zavaleta, C. L. *et al.* A Raman-based endoscopic strategy for multiplexed molecular imaging. *Proc. Natl Acad. Sci. U. S. A.* **110**, E2288–E2297 (2013).
A fibre-based Raman device that could be inserted through a clinical endoscope was developed and demonstrated the ability to detect up to ten labelled nanosensors via SERS with excellent sensitivity.
- 125 Funovics, M. A., Alencar, H., Montet, X., Weissleder, R. & Mahmood, U. Simultaneous fluorescence imaging of protease expression and vascularity during murine colonoscopy for colonic lesion characterization. *Gastrointest. Endosc.* **64**, 589–597 (2006).
- 126 Zavaleta, C. L. *et al.* Preclinical evaluation of Raman nanoparticle biodistribution for their potential use in clinical endoscopy imaging. *Small* **7**, 2232–2240 (2011).
- 127 Thakor, A. S. *et al.* Oxidative stress mediates the effects of Raman-active gold nanoparticles in human cells. *Small* **7**, 126–136 (2011).
- 128 Thakor, A. S. *et al.* The fate and toxicity of Raman-active silica-gold nanoparticles in mice. *Sci. Transl. Med.* **3**, 79ra33 (2011).
- 129 Jeong, S. *et al.* Fluorescence–Raman dual modal endoscopic system for multiplexed molecular diagnostics. *Sci. Rep.* **5**, 9455 (2015).
- 130 Wang, Y. W., Kang, S., Khan, A., Bao, P. Q. & Liu, J. T. C. *In vivo* multiplexed molecular imaging of esophageal cancer via spectral endoscopy of topically applied SERS nanoparticles. *Biomed. Opt. Express* **6**, 3714–3723 (2015).
- 131 Garai, E. *et al.* A real-time clinical endoscopic system for intraluminal, multiplexed imaging of surface-enhanced Raman scattering nanoparticles. *PLoS One* **10**, e0123185 (2015).
A unique endoscopic opto-electro-mechanical Raman device was the first device to allow SERS imaging of tissue during gastrointestinal endoscopy.
- 132 Stone, N., Faulds, K., Graham, D. & Matousek, P. Prospects of deep Raman spectroscopy for noninvasive detection of conjugated surface enhanced resonance Raman scattering nanoparticles buried within 25 mm of mammalian tissue. *Anal. Chem.* **82**, 3969–3973 (2010).
This study was the first to report the technique of surface enhanced spatially offset Raman spectroscopy (SESORS).
- 133 Stone, N. *et al.* Surface enhanced spatially offset Raman spectroscopic (SESORS) imaging — the next dimension. *Chem. Sci.* **2**, 776–780 (2011).
- 134 Xie, H. N. *et al.* Tracking bisphosphonates through a 20 mm thick porcine tissue by using surface-enhanced spatially offset Raman spectroscopy. *Angew. Chem. Int. Ed.* **51**, 8509–8511 (2012).
- 135 Sharma, B., Ma, K., Glucksberg, M. R. & Van Duyne, R. P. Seeing through bone with surface-enhanced spatially offset Raman spectroscopy. *J. Am. Chem. Soc.* **135**, 17290–17293 (2013).
- 136 Hubert, C. A. (Google Patents, 1971).
- 137 Lyandres, O. *et al.* Progress toward an *in vivo* surface-enhanced Raman spectroscopy glucose sensor. *Diabetes Technol. Ther.* **10**, 257–265 (2008).
- 138 *FreeStyle Libre*, <<https://www.freestylelibre.co.uk/>> (Accessed 2017).
- 139 *DEXCOM Continuous Glucose Monitoring*, <<https://www.dexcom.com/continuous-glucose-monitoring>> (Accessed 2017).

- 140 Shafer-Peltier, K. E., Haynes, C. L., Glucksberg, M. R. & Van Duyne, R. P. Toward a glucose biosensor based on surface-enhanced Raman scattering. *J. Am. Chem. Soc.* **125**, 588–593 (2003).
- 141 Lyandres, O. *et al.* Real-time glucose sensing by surface-enhanced Raman spectroscopy in bovine plasma facilitated by a mixed decanethiol/mercaptohexanol partition layer. *Anal. Chem.* **77**, 6134–6139 (2005).
- 142 Qi, G. *et al.* Glucose oxidase probe as a surface-enhanced Raman scattering sensor for glucose. *Anal. Bioanal. Chem.* **408**, 7513–7520 (2016).
- 143 Maiti, K. K. *et al.* Development of biocompatible SERS nanotag with increased stability by chemisorption of reporter molecule for *in vivo* cancer detection. *Biosens. Bioelectron.* **26**, 398–403 (2010).
- 144 Maiti, K. K. *et al.* Multiplex targeted *in vivo* cancer detection using sensitive near-infrared SERS nanotags. *Nano Today* **7**, 85–93 (2012).
- 145 Mallia, R. J., McVeigh, P. Z., Fisher, C. J., Veilleux, I. & Wilson, B. C. Wide-field multiplexed imaging of EGFR-targeted cancers using topical application of NIR SERS nanoprobes. *Nanomedicine* **10**, 89–101 (2015).
- 146 Sinha, L. *et al.* Quantification of the binding potential of cell-surface receptors in fresh excised specimens *via* dual-probe modeling of SERS nanoparticles. *Sci. Rep.* **5**, 8582 (2015).
- 147 Kircher, M. F. *et al.* A brain tumor molecular imaging strategy using a new triple-modality MRI-photoacoustic-Raman nanoparticle. *Nat. Med.* **18**, 829–834 (2012).
- The design of a novel nanoprobe which allows imaging using three different techniques, combining their advantages for successful brain tumour resection.**
- 148 Sershen, S. R., Westcott, S. L., Halas, N. J. & West, J. L. Temperature-sensitive polymer-nanoshell composites for photothermally modulated drug delivery. *J. Biomed. Mater. Res.* **51**, 293–298 (2000).
- 149 Huschka, R. *et al.* Light-induced release of DNA from gold nanoparticles: nanoshells and nanorods. *J. Am. Chem. Soc.* **133**, 12247–12255 (2011).
- 150 Huo, S. *et al.* Ultrasmall gold nanoparticles as carriers for nucleus-based gene therapy due to size-dependent nuclear entry. *ACS Nano* **8**, 5852–5862 (2014).
- 151 Mackanic, D. G., Mabbott, S., Faulds, K. & Graham, D. Analysis of photothermal release of oligonucleotides from hollow gold nanospheres by surface-enhanced Raman scattering. *J. Phys. Chem. C* **120**, 20677–20683 (2016).
- 152 Cheng, Y. *et al.* Highly efficient drug delivery with gold nanoparticle vectors for *in vivo* photodynamic therapy of cancer. *J. Am. Chem. Soc.* **130**, 10643–10647 (2008).
- 153 Xia, Y. *et al.* Three dimensional plasmonic assemblies of AuNPs with an overall size of sub-200 nm for chemo-photothermal synergistic therapy of breast cancer. *Nanoscale* **8**, 18682–18692 (2016).
- 154 Kang, B., Afifi, M. M., Austin, L. A. & El-Sayed, M. A. Exploiting the nanoparticle plasmon effect: observing drug delivery dynamics in single cells *via* Raman/fluorescence imaging spectroscopy. *ACS Nano* **7**, 7420–7427 (2013).
- 155 Gao, Y. *et al.* Multifunctional gold nanostar-based nanocomposite: synthesis and application for noninvasive MR-SERS imaging-guided photothermal ablation. *Biomaterials* **60**, 31–41 (2015).

[H1] Acknowledgements

KF and SL thank the Leverhulme Trust for financial support through Research Project Grant RPG-2012-758.

[H1] Competing interests statement

The authors declare no competing interests.

[H1] Publisher's note

Springer Nature remains neutral with regard to jurisdictional claims in published maps and institutional affiliations.

[H1] How to cite this article

Phan, N. T. N., Li, X. & Ewing, A. G. Measuring synaptic vesicles using cellular electrochemistry and nanoscale molecular imaging. *Nat. Rev. Chem.* **1**, xxxxx (2017).

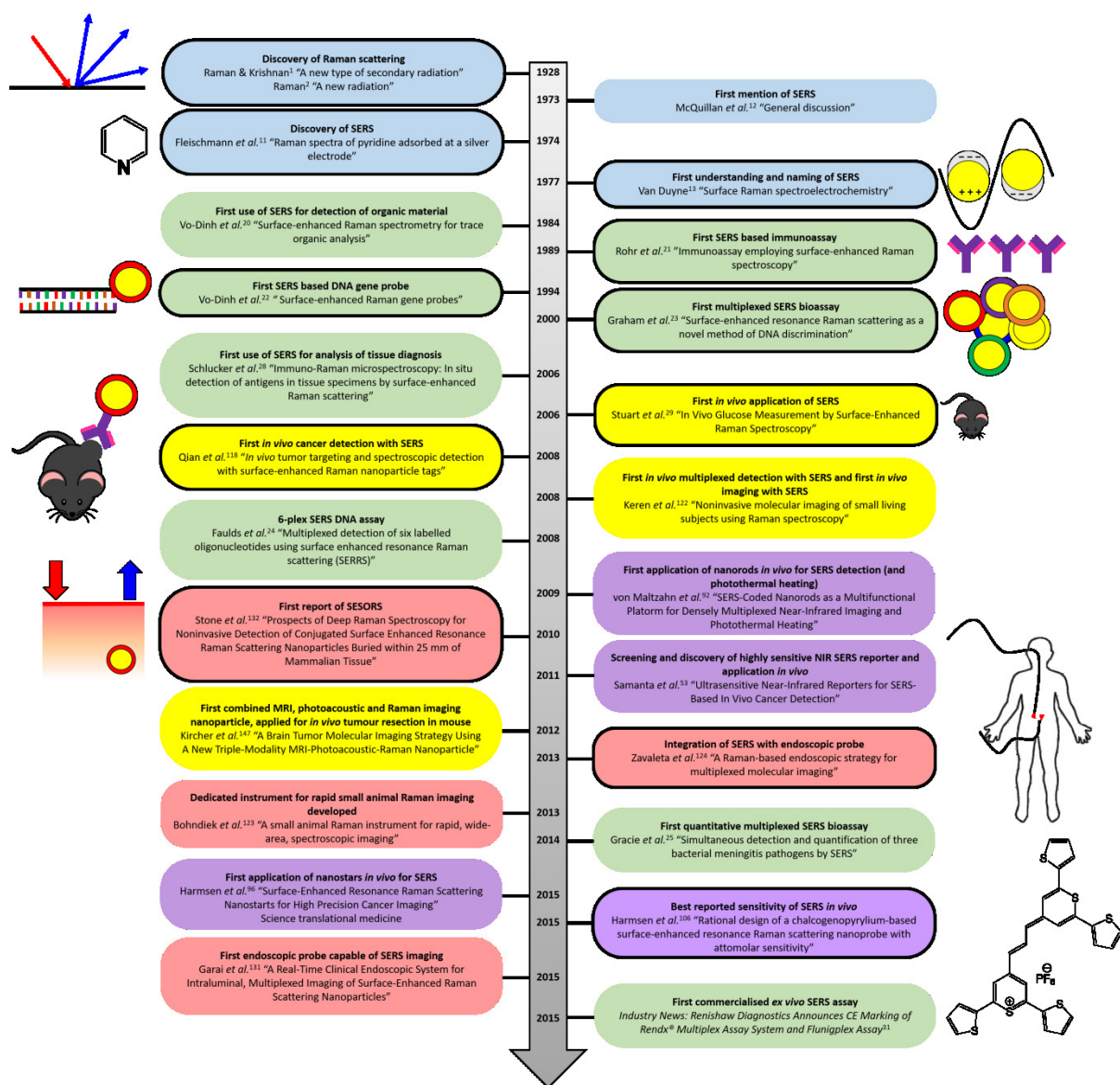


Figure 1 | **Some key developments in SERS research for *in vivo* applications.** The most prominent advances are outlined in black. Advancements in understanding Raman and SERS (blue), developing *ex vivo* SERS for biological analysis (green), designing nanoprobe for *in vivo* biosensing (purple), applying SERS *in vivo* (yellow), and SERS instrumentation (red), are presented in their respective colours. SERS, surface enhanced Raman scattering; NIR, near-infrared; LSPR, localized surface plasmon resonance; HGNs, hollow gold nanoshells; SESORS, surface enhanced spatially offset Raman scattering; MRI, magnetic resonance imaging.

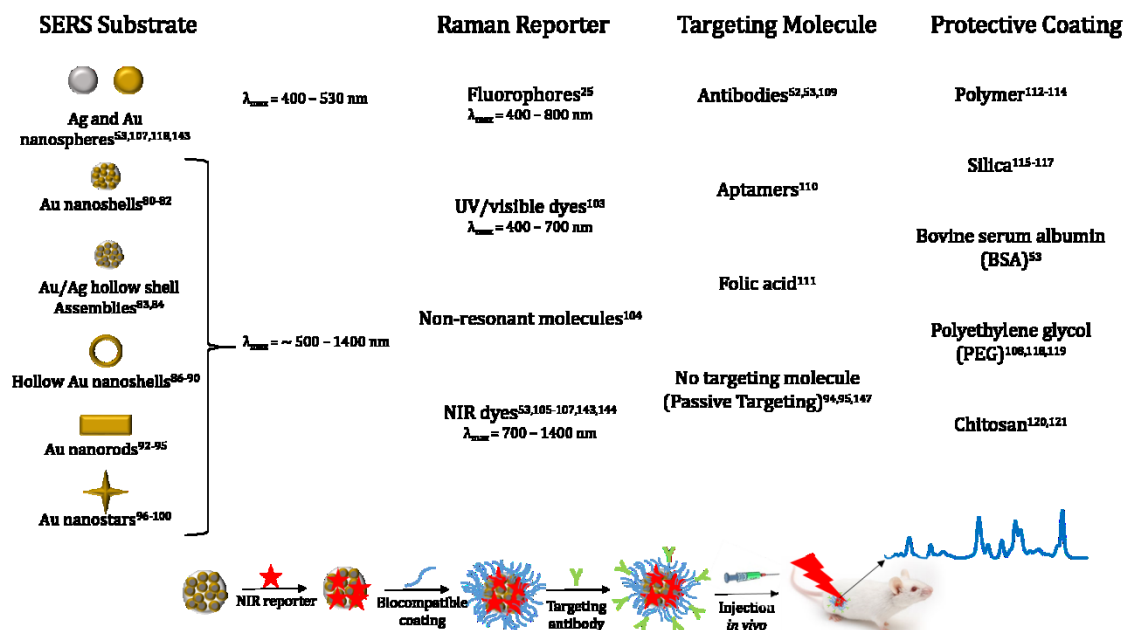


Figure 2 | *In vivo* SERS makes use of nanosensors, each of which typically features a signal-enhancing metal substrate, a Raman reporter, an analyte-targeting molecule and a protective coating. Examples are given for each component, with the absorption maxima λ_{max} given for the substrates and Raman reporters, highlighting the most suitable choices for NIR-SERS.

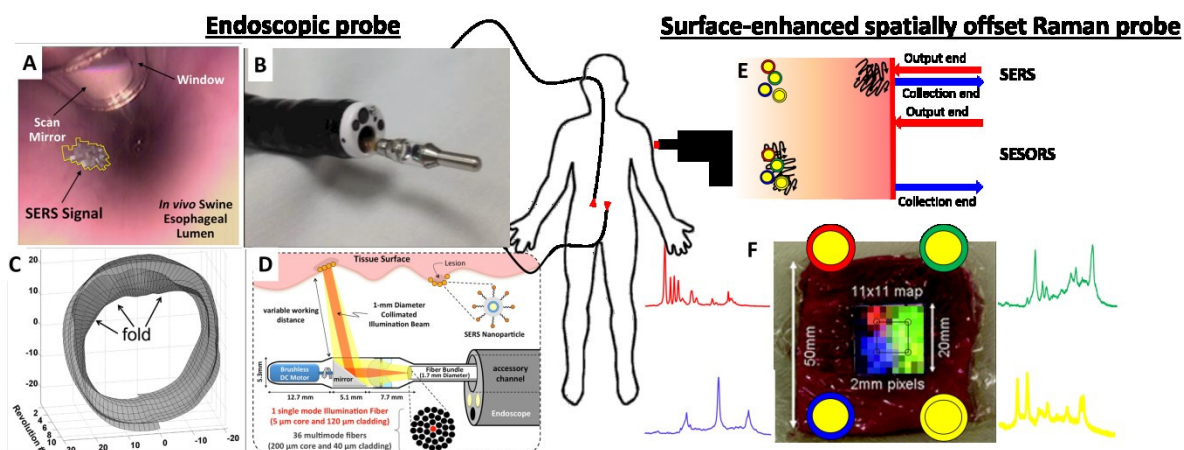


Figure 3 | **State-of-the-art instrumentation and experimental configurations used to conduct SERS biosensing *in vivo*.** **a** | A white light image from a uniquely designed endoscopic probe with Raman accessory that enables rapid imaging inserted into a pig oesophagus with superimposed SERS signal corresponding to ratiometric SERS signal from two nanoparticle types used to account for non-specific binding¹³¹. **b** | The gastrointestinal tract is easily accessed using endoscopic probes, through which fibre-optic Raman probes can be inserted. **c** | A 3D construction of colon topography generated using Raman background signals acquired using this device in a human. **d** | The Raman endoscopic probe detects cancer by locating SERS nanoparticles, which recognize cancer-specific antigens and localize at tumour sites. The probe has a single illumination fibre and 36 multimode collection fibres. A brushless motor rotates a mirror through 360° to image the colon wall. **e** | By comparison, SESORS measurements use a probe outside the body, with light being collected from a region offset from the illumination point. This new method enables detection of probes buried more deeply than those detectable by SERS. **f** | SESORS is amenable to multiplexed detection of four different SERS probes in porcine tissue¹³³. Panels **a–d** are reproduced from REF. 131, PLOS. Panels **e** and **f** are reproduced from REF. 133, Royal Society of Chemistry.

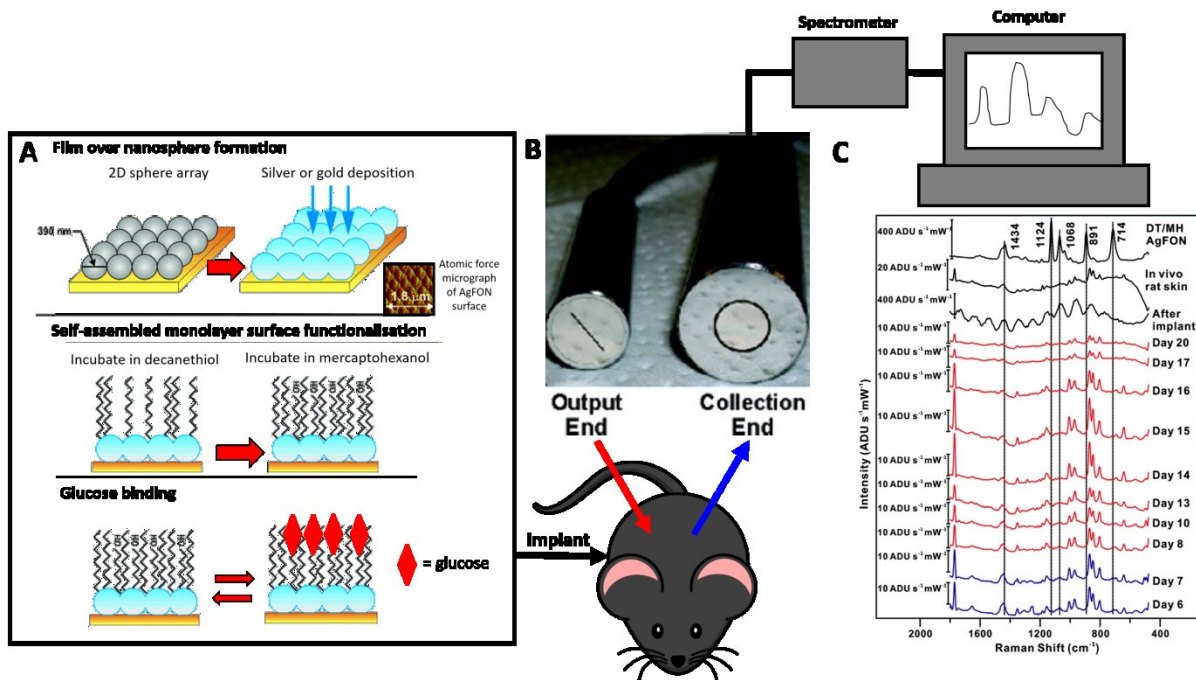


Figure 4 | *In vivo* glucose monitoring using implanted SERS probe and SESORS detection. **a** | SERS-based glucose quantitation makes use of a nanosphere array, over which is deposited a Ag or Au film. Such a ‘film over nanosphere’ (FON) surface then is decorated with a self-assembled monolayer (SAM) using decanethiol and mercaptohexanol, which acts to bind glucose near the FON surface.¹⁴¹ **b** | An Ag-coated sample (AgFON) was inserted subcutaneously into a rat and SERS spectra were acquired using a SESORS probe.⁴⁸ **c** | Spectra of functionalised AgFON, rat skin with and without implanted SERS probe, and the response 6 to 20 days after insertion. Panel **a** is adapted from REF. 141, American Chemical Society. Panel **b** is reproduced from REF. 48, American Chemical Society. Panel **c** is reproduced from REF. 51, American Chemical Society.

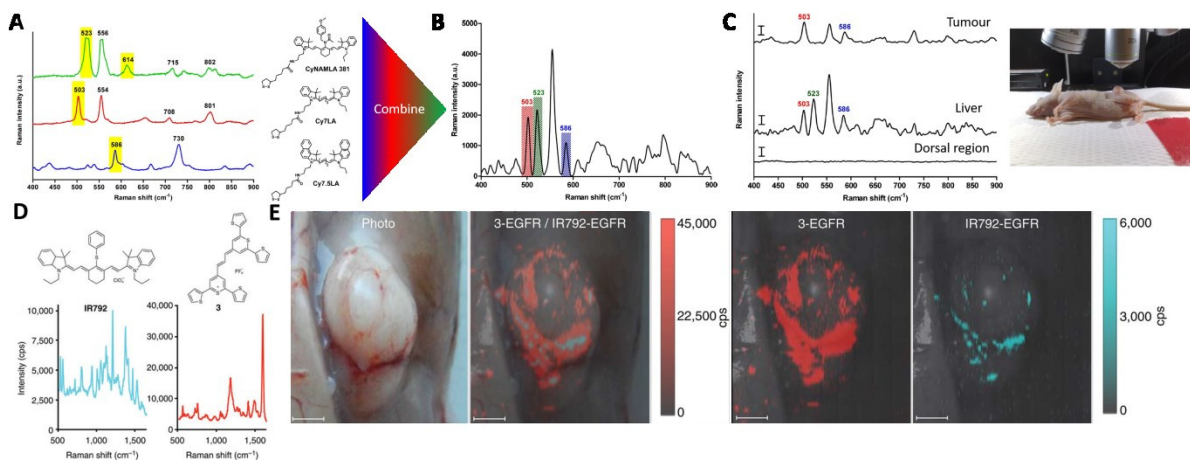


Figure 5 | *In vivo* cancer detection using near-infrared optimized SERS probes. **a** | Raman spectra of three SERS probes optimized for NIR detection ($\lambda_{\text{ex}} = 785 \text{ nm}$, 60 mW laser power, 10 s acquisition). The probes are based on Au NPs, onto which the cyanine reporters CyNAMLA 381, Cy7LA and Cy7.5LA are chemically adsorbed. The bands highlighted in yellow are the most characteristic¹⁴⁴. **b** | A living mouse was injected with the three probes in bovine serum albumin, with the entire chromophores making their way into the liver. Localization is evident on considering the multiplexed SERS spectrum, which features bands characteristic of each probe (red = Cy7LA, green = CyNAMLA 381, blue = Cy7.5LA ($\lambda_{\text{ex}} = 785 \text{ nm}$, 30 mW laser power, 20 s acquisition)). **c** | The AuNPs bearing Cy7LA and Cy7.5LA reporters were conjugated to anti-EGFR antibodies, while those bearing CyNAMLA 381 were functionalized with anti-HER2. The three probes were injected into the

tail vein of a living xenograft mouse model with a tumour formed from oral squamous cell carcinoma cells, which show high EGFR and low HER2 expression. SERS spectra were acquired from tumour, liver and dorsal sites of the mouse and indicated that only the EGFR-targeting probes were detected in the tumour site, all probes were detected in liver and no probes were detected at the dorsal site (scale bar = 2000 counts; $\lambda_{ex} = 785$ nm, 30 mW laser power, 20 s acquisition). **d** | Structure and SERS spectra of the reporter IR792 (cyan, 1.0 fM detection limit), as well as a recently developed ultrabright NIR chalcogenopyrylium dye (red, 0.1 fM detection limit)¹⁰⁶, both of which were attached to the surface of 60 nm AuNPs and coated with a 15 nm SiO₂ layer. **e** | The dye-conjugated AuNPs were functionalized with an EGFR-targeting antibody, and intravenously injected into mice with A431 xenograft tumours (each probe was at a concentration 15 fmol g⁻¹), which were imaged 18 h after injection ($\lambda_{ex} = 785$ nm, 10 mW laser power, 1.5 s acquisition, 5 \times objective). A white light image of the tumour site is shown, along with overlaid false colour images of each reporter generated using a direct classical least squares algorithm both separately and with the dyes overlaid. Signals for the chalcogenopyrylium nanoprobe (red) were approximately 3 \times more intense than those for IR792 nanoprobe (cyan). Scale bars = 2 mm. Panels **a–c** are reproduced from REF. 144, American Chemical Society. Panels **d** and **e** are reproduced from REF. 106, Nature Research.

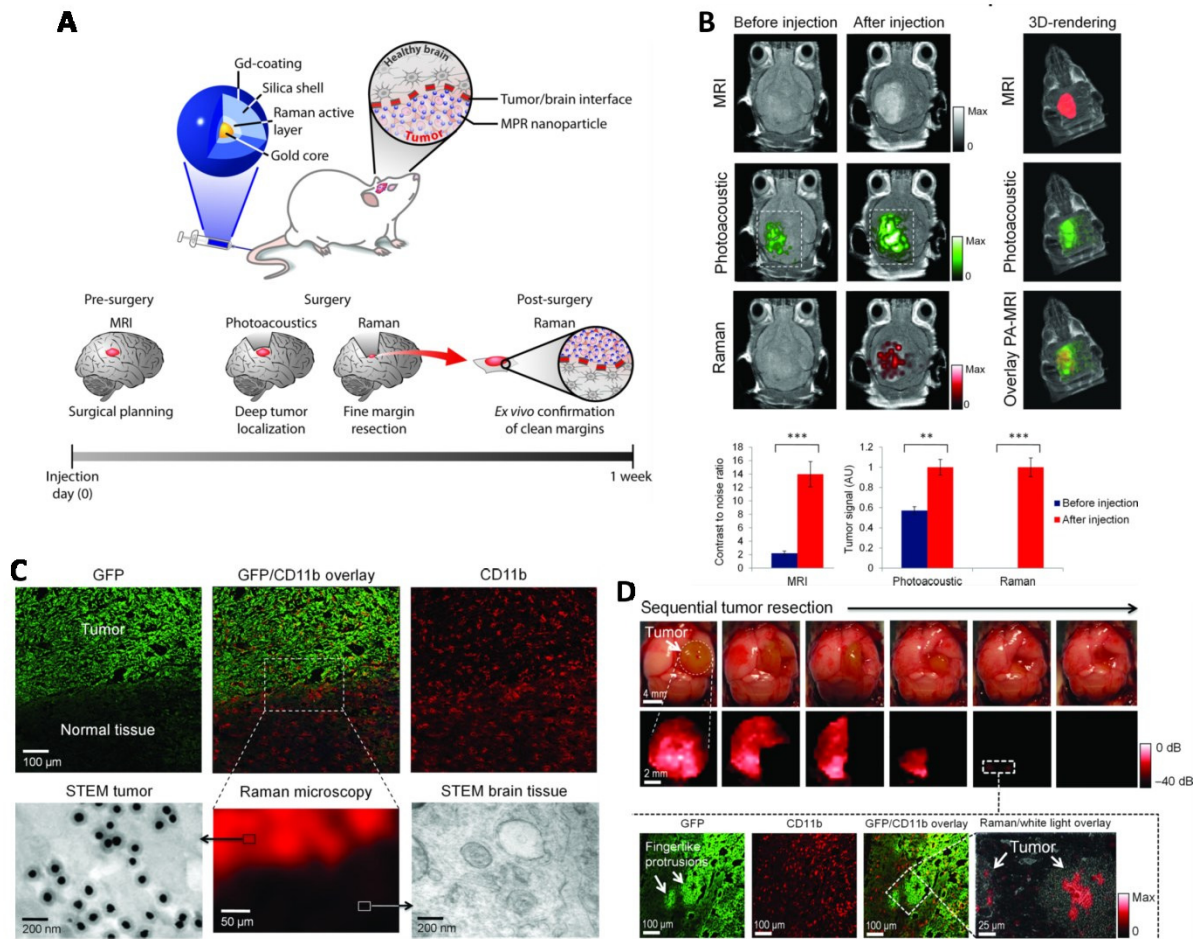


Figure 6 | Brain tumour imaging and guided tumour resection using triple modality nanoparticles. **Aa** | MPR nanoprobe are based on AuNPs functionalized with a Raman reporter, on top of which is applied a SiO₂ coating and a Gd(III) MRI contrast agent. The probes are injected into the tails of tumour-bearing mice and accumulate in the tumour without passing into healthy tissue¹⁴⁷. **Ab** | Clinical use would involve initially locating the tumour using MRI, after which photoacoustic imaging can guide tumour resection. Raman can then be used to guide removal of residual tumour and for subsequent examination of samples *ex vivo*. **Ba** | Photoacoustic, Raman and magnetic resonance images of the brain (skin and skull intact) acquired before (2D) and 2, 3 and 4 h after (2D and 3D)

injection. **Bb** | Quantification of acquired signal for each imaging method before and after injection of MPR nanoparticles. **Ca** | Sections from an eGFP+U87MG brain tumour, stained with enhanced green fluorescence protein (eGFP, green) to visualize the tumour margins and CD11b (red) to visualize glial cells, examined by laser scanning confocal microscopy. **Cb** | An adjacent slice was imaged using Raman to visualize MPR biodistribution. Raman signals were obtained from the eGFP+ cells, indicating the presence of the probe in the tumour but not in the adjacent healthy tissue. Scanning transmission electron microscopy (STEM) images verified the presence of MPRs in the brain tissue, while no MPRs were seen in the healthy brain tissue. **Da** | Photographs and Raman images after each step of the tumour resection. Following bulk removal of the tumour, small areas of Raman signal were still observed (outlined by dashed white box). **Db** | Histological analysis of these areas showing finger-like protrusions extending into the surrounding tissue. Raman signal was obtained from these areas due to the accumulation of the MPRs. Figure reproduced from REF. 147, Nature Research.

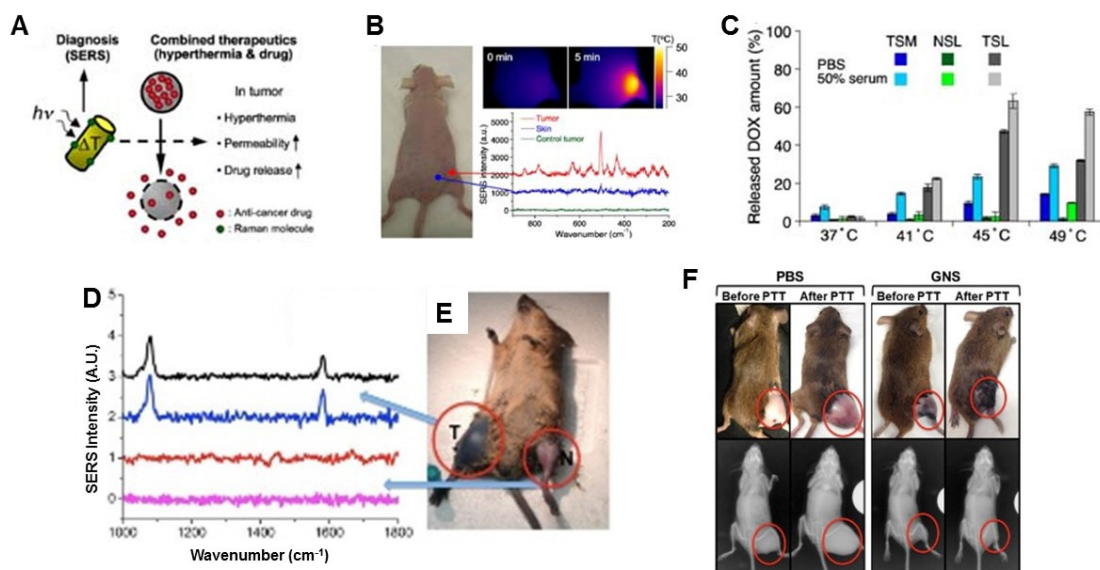


Figure 7 | **Nanoparticles and SERS for drug delivery and photothermal therapy *in vivo*.** **a** | Nanoparticles are useful both in terms of detecting a disease using SERS (diagnostics), as well as treating it by releasing a drug or thermal energy (therapeutics). Such multifunctional nanoprobe are thus known as theranostic agents.⁹⁵ **b** | Probes based on gold nanorods (AuNRs) can be injected into a tumour-bearing mouse, which can be imaged optically, thermally, and spectroscopically (by interrogating a Raman reporter).⁹⁵ The IR thermal maps shown were obtained immediately before (left) and 5 min after (right) irradiation with a diode laser ($\lambda_{\text{ex}} = 810 \text{ nm}$, 0.75 W cm^{-2}). Raman spectra ($5 \times 60 \text{ s}$ acquisitions) were acquired from the tumour region (red trace) and from skin near the tumour (blue trace).⁹⁵ **c** | The AuNRs can be loaded with doxorubicin (DOX) prior to being protected by a thermally sensitive liposome (TSL), control liposome with no thermal sensitivity (NSL) or a thermally sensitive micelle (TSM). The three samples are incubated with cells for 10 min at different temperatures, after which the amount of DOX released *in vitro* is quantified using fluorescence spectroscopy.⁹⁵ **d** | *In vivo* SERS spectra of 30 nm (blue and pink) and 60 nm (black and red) gold nanostar (AuNS) nanoprobe with 4-mercaptopbenzoic acid SAMs.¹⁰⁰ Characteristic SERS peaks can be detected at 1067 and 1588 cm^{-1} in the tumour, but not in the normal muscle. **e** | Mouse with primary sarcomas 3 days after dosing with 30 nm AuNS.¹⁰⁰ Significant AuNS accumulation can be seen in the tumour (T), but not in the normal leg muscle (N) of the contralateral leg. **f** | Photographs (top) and X-ray images (bottom) of mice before and after photothermal therapy with tumours circled in red.¹⁰⁰ The control mouse images were taken 7 days after treatment and the images of the mouse with AuNS injection were taken 3 days after treatment. Dark discoloration in the tumour region for the AuNS mouse is due to nanoparticle accumulation in the underlying tumour. X-ray images show a clear decrease in tumour bulk for the mouse with AuNS injection, but a significant increase in tumour

size for the mouse with buffer (PBS) injection. Panel **a** is adapted, and panels **b** and **c** are reproduced from REF. 95, Wiley. Panels **d–f** are reproduced from REF. 100, Ivyspring International.

[H1] Subject categories

Physical sciences / Chemistry / Analytical chemistry / Imaging studies

[URI /639/638/11/942]

Physical sciences / Chemistry / Analytical chemistry / Bioanalytical chemistry

[URI /639/638/11/872]

Physical sciences / Chemistry / Analytical chemistry / Medical and clinical diagnostics

[URI /639/638/11/876]

[H1] ToC blurb

Surface enhanced Raman scattering (SERS) is a physical phenomenon first discovered in 1974, which has since been exploited for bioanalysis due to its high sensitivity and multiplexing capabilities. We Review current progress and the steps required for SERS to realise its full potential for *in vivo* application in humans.